ARC Centre of Excellence in Population Ageing Research

Working Paper 2020/04

Financial Engineering: A Flexible Longevity Bond to Manage Individual Longevity Risk

Yuxin Zhou, Michael Sherris, Jonathan Ziveyi and Mengyi Xu

Financial Engineering: A Flexible Longevity Bond to Manage Individual Longevity Risk

Yuxin Zhou*, Michael Sherris†, Jonathan Ziveyi‡and Mengyi Xu§

April 20, 2020

Abstract

There is a significant potential demand in many countries around the world for a flexible product to manage individual longevity risk arising from the prevalence of defined contribution pensions, uncertainty in improvements in life expectancy, potential reductions in public pensions and a lack of suitable longevity insurance products. The classical insurance product to manage individual longevity risk is the life annuity. Annuity markets remain thin, driven by many factors including lack of transparency in pricing, high product loadings, bequest motives, lack of liquidity and loss aversion. This paper proposes an individual longevity bond, not currently available, as a combined investment and insurance product to allow individuals to flexibly manage their longevity risk. The bond is a post-retirement product that combines a lifetime income along with a flexible death benefit to meet bequest and liquidity needs. The longevity bonds are issued through a special purpose vehicle which is fully collateralized with a fixed interest portfolio. We apply financial and actuarial models and techniques that provide transparent pricing for interest rate and mortality risk, the construction of optimally immunized bond portfolios and the determination of a loading and solvency margin for systematic longevity risk. We also quantify the natural hedging benefits of the individual bond cash flows arising from the flexible inclusion of both survival dependent income benefits and mortality dependent bequest benefits payable on death.

Working Paper

Keywords: longevity risk, stochastic mortality, longevity bond, immunization, natural hedging

JEL Classification Numbers: G11, G22, G23, C53, C58, C61

*School of Risk & Actuarial Studies, Australian Research Council Centre of Excellence in Population Ageing Research (CEPAR), UNSW Sydney, email: yuxin.zhou@unsw.edu.au

†School of Risk & Actuarial Studies, CEPAR, UNSW Sydney, email: m.sherris@unsw.edu.au

‡School of Risk & Actuarial Studies, CEPAR, UNSW Sydney, email: j.ziveyi@unsw.edu.au

§School of Risk & Actuarial Studies, CEPAR, UNSW Sydney, email: m.xu@unsw.edu.au

1 Introduction

Longevity risk is the risk that individuals may live longer than expected and consequently outlive their retirement savings. It is one of the most significant risks that individuals face under a defined contribution (DC) pension system, which has become dominant in many countries, including Australia where more than 87% of pension assets are in DC funds (Willis Towers Watson, 2018). The traditional product for individuals to manage longevity risk is the life annuity. Classical economic theory suggests that individuals with no bequest motive will maximize their expected lifetime utility by fully annuitizing their wealth (Yaari, 1965). Despite this, empirical evidence shows that life annuity markets are thin. This has become known as the 'annuity puzzle', a term coined in Modigliani (1986).

There are many explanations given for the 'annuity puzzle' covering a combination of demand side and supply side reasons. Demand side reasons include: high loadings to allow for adverse selection, bequest motives, loss aversion for early death, and liquidity (Brown, 2009). Supply side reasons include: high interest rate risk, longevity risk created by the long duration of life annuities, and the difficulty to find a suitable asset on the market to hedge interest rate and longevity risks (Evans and Sherris, 2010).

Longevity bonds have mostly been proposed for insurers to hedge the longevity risk exposure from issuing life annuities (Blake and Burrows, 2001). These include coupon-at-risk and principal-at-risk longevity bonds (Blake et al., 2006). In contrast, little attention has been given to developing longevity bonds for individuals to manage their longevity risk. The SM bond proposed in De Jong and Ferris (2019), which links the principal payment to individual survivorship, is a recent example. For this bond, the principal payment is lost if the bondholder dies before the bond matures, and it goes into a pool for bondholders to share at maturity. By purchasing these bonds each year before retirement, individuals receive retirement income in each year after retirement as the principal payment on the bond matures, provided they are alive. This aims to replicate the income pattern of a DB plan. The bond generates retirement income as part of an investment strategy for contributions before retirement and relies on a pooling mechanism for longevity risk as well as a market pricing mechanism for this risk.

Our focus is an individual longevity bond not available currently in the market that allows individuals to flexibly manage their longevity risk taking into account their preference for income and bequests. The bond is an investment product which combines a flexible death benefit with an income based survival benefit to address the limitations of a life annuity, particularly the bequest motive, loss aversion and high loadings. The survival benefit is a monthly coupon payment while the individual is alive, and the death benefit is the principal which is fully or partially returned in the event of death. The coupon payments hedge the individual's longevity risk, and the death benefit meets bequest motives and reduces loss aversion in the event of early death. Importantly, individuals have the flexibility to structure a bond that meets their preferences through different combinations of a survival income benefit and a death benefit. The individual bonds are issued through a special purpose vehicle (the issuer), which in Australia would hold a life insurer license, but could be backed by a reinsurer, that aggregates and manages the interest rate and mortality risks.

Recent developments in continuous-time mortality models have extended the term structure affine models of interest rates to systematic mortality (Dahl, 2004; Biffis, 2005; Schrager, 2006; Luciano et al., 2012). They allow a consistent modeling approach for interest rate and mortality risk in financial and insurance applications. Most of these models use age-period mortality data and are single cohort models. Blackburn and Sherris (2013) present and assess consistent age-period single cohort affine mortality models including estimation methodology and demonstration of parameter stability across time in the models. Cohort effects are important in

mortality models. Xu et al. (2019) extend affine mortality models to multi-cohorts by including a cohort-specific factor in an age-period mortality model and include a financial application to assess a price of risk in the models.

We propose and apply a financial engineering valuation and immunizing framework for the individual longevity bond based on the Arbitrage-Free Nelson Siegel (AFNS) models for both interest rates and mortality rates. Huang et al. (2019) extend and assess AFNS age-cohort mortality models by calibrating the models to age-cohort mortality data, provide a comparison of a range of affine mortality models, and demonstrate the benefits of the independent AFNS mortality model. The AFNS models are designed for financial and insurance applications. In practice, the Gaussian AFNS mortality models have been to shown to have very low probabilities of negative mortality rates (Huang et al., 2019), one of the theoretical limitations of the models. Our longevity bonds are cohort based so we use AFNS models for both interest rates and age-cohort mortality calibrated to Australian data.

Luciano et al. (2012) apply affine models to the delta-gamma hedging of interest rate and mortality risk of a range of mortality-linked insurance contracts. Liu and Sherris (2017) apply the immunization theory presented in Panjer et al. (1998) to a life annuity portfolio, and use linear programming with a mean-absolute deviation constraint in order to optimally match the asset and liability expected cash flows including Fisher-Weil duration. They show the benefits of this approach over delta-gamma hedging.

We use the approach in Liu and Sherris (2017) to derive, compare and assess immunized bond portfolios for the individual longevity bonds using Australian government bonds to minimize the interest rate risk. We compare the effectiveness of both coupon paying bonds and hypothetical annuity bonds in immunizing the individual longevity bonds. We use Australian data and Australian fixed interest bonds, but the results and methodology applies to any developed market with the need for post-retirement products and an active bond market.

We price the aggregate mortality risk using Australian population mortality. Since there are no longevity-linked bonds in Australia, the issuer holds capital for the risk not hedged by the immunized bond portfolio, which is mainly the systematic longevity risk. The cost of holding this capital is quantified using a Solvency II approach and determines a risk margin as a proportion of the bond price. Our immunization and risk analysis takes into account systematic mortality risk for age-cohort population mortality. In practice, different mortality assumptions would need to be considered for the different types of individual longevity bonds reflecting potential adverse selection. Our focus is on the systematic longevity risk. Our proposed individual longevity bond has both survival and death benefits, and since an individual's bequest motive is expected to result in a mix of these, the effects of adverse selection are reduced.

For the individual longevity bonds, the value of the death benefit provides a natural hedge for the value of the survival income benefit as systematic mortality changes occur. The proposed longevity bond with a coupon payment as survival income and principal as a death benefit is shown to have significant natural hedging, resulting in more effective pricing and reduced capital requirements. We quantify this natural hedging effect based on the final year surplus of the immunized portfolio and the reduction in capital cost compared to the longevity bond with a survival income benefit only. As is commonly used for longevity risk, and reflecting Solvency II requirements, we use Value-at-Risk (VaR) as a risk measure.

Our contributions focus on the financial engineering underlying individual longevity bonds including the interest rate and age-cohort mortality models, the construction and assessment of the government bond portfolios used to immunize the individual longevity bonds, quantifying the capital costs for the systematic longevity risk and assessing the natural hedging benefits that are a feature of the individual longevity bonds.

The remainder of this paper is structured as follows. Section 2 covers the proposed design of the individual longevity bonds to meet individual needs for income, bequest and payments on death. Section 3 presents the AFNS interest rate and mortality models, including model simulation results. Section 4 presents the method for construction of the immunized government bond hedging portfolio with coupon and annuity bonds, and assesses the hedging performance for the individual longevity bonds by considering the final year surplus distribution for the immunized portfolio. Section 5 presents the methodology for determining the solvency capital requirements of the residual risk from issuing the individual longevity bonds, and determines the cost of holding capital for the individual longevity bonds. Section 6 concludes with a discussion of the main findings and implications.

2 Individual Longevity Bond Designs

Our proposal is for a flexible individual longevity bond design structured as an investment product incorporating longevity insurance features. The bond incorporates a flexible choice of survival benefits $\mathcal{S}$, as bond coupon income, and death benefits $\mathcal{D}$, as a bequest or liquidity preference. The bonds are a combination of a lifetime coupon and principal bond that returns the initial bond price on death and an annuity bond that replicates the classic life annuity. Individuals select a weighted combination of these bonds to provide a flexible bond structure that allows for individual preferences for survival income and bequest death benefit.

The general structure of the bond payoffs is represented as:

- Monthly payments $\mathcal{S}$ while the individual is alive as the survival benefit.
- Death payment $\mathcal{D}$ at the end of the month τ in which the individual dies.

All the bonds are standardized to a price of 100 at the time of issue. Pricing of the bonds is covered later.

2.1 Longevity Bond Structure: Lifetime Coupon and Principal Bond

The individual longevity bond structure referred to as the lifetime coupon and principal bond (LCP Bond) has a monthly survival income benefit $\mathcal{S}^{LCP}$, which is the coupon payment based on the principal $\mathcal{D}^{LCP}$,

$$\mathcal{S}^{LCP} = \frac{r_c}{12} \times \mathcal{D}^{LCP},$$

where r_c stands for the annual coupon rate. The coupon rate is set to be 2% for illustration reflecting the current low interest rates. This interest rate reflects the term structure of interest rates and a mortality credit. The principal $\mathcal{D}^{LCP}$ is paid at the end of the month τ in which the individual dies. The timeline of the payoffs for an individual who purchases the bond is displayed below, with time measured in years:

2.2 Longevity Bond Structure: Lifetime Annuity Income Bond

The individual longevity bond structure referred to as the lifetime annuity income bond (LAI Bond) has a payoff similar to a life annuity. The monthly survival benefit $\mathcal{S}^{LAI}$ is constant over

time, and there is no principal payment in the event of death. The time-line of the payoffs for an individual who purchases the bond is displayed below:

2.3 Longevity Bond Structure 3: Flexible Lifetime Income and Principal Bond Series W%

The main individual bond structure is the flexible lifetime income and principal bond series $W\%$ (Flexible LIP Bond^W). It is a mix of $W\%$ of the LCP Bond and $(1-W\%)$ of the LAI Bond. An individual who purchases this bond has the flexibility to choose the weight W, thus balancing their preferences between the survival benefit and the death benefit to take into account bequest motives.

The survival benefit $\mathcal{S}^W$ and death benefit $\mathcal{D}^W$ of this bond are represented as:

$$\begin{aligned}\mathcal{S}^W &= W\% \cdot \mathcal{S}^{LCP} + (1 - W\%) \cdot \mathcal{S}^{LAI},\\ \mathcal{D}^W &= W\% \cdot \mathcal{D}^{LCP} + (1 - W\%) \cdot \mathcal{D}^{LAI} = W\% \cdot \mathcal{D}^{LCP}.\end{aligned}$$

The timeline of the payoffs for an individual who purchases the bond is displayed below:

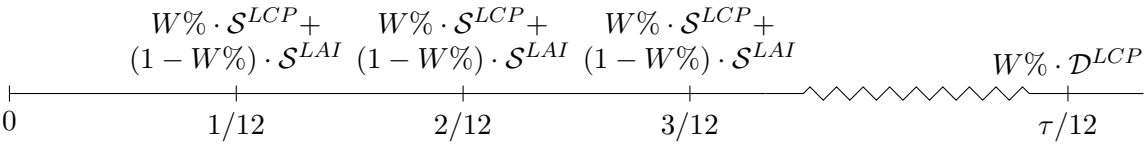

Most individuals are expected to select a flexible bond with weight $W\%$ reflecting their bequest motives. Since this bond is a weighted combination of the LCP Bond and the LAI Bond, we can construct our immunizing portfolios and price aggregate mortality risk for these two bonds and the flexible bond results are a weighted combination of the results for these two bonds. Since both the LCP Bond and LAI Bond are standardized to the price of 100 at the time of issue, the price of the Flexible LIP Bond^W is always 100 regardless of the value of W.

3 Financial Engineering - Interest Rate and Systematic Mortality Models

To price and determine immunizing government bond portfolios for the individual longevity bonds we present, estimate and assess Arbitrage-Free Nelson-Siegel interest rate and mortality models calibrated with Australian data. Section 3.2 outlines the general framework of the affine models. The estimation and simulation results of the AFNS interest rate and systematic mortality models are provided in Section 3.3 and 3.4, respectively. Interest rates are modeled using an Arbitrage-Free Nelson-Siegel (AFNS) model proposed in Christensen et al. (2011) that has both theoretical and empirical support for application to bond valuation. The AFNS affine model is adapted to model systematic mortality rates in Huang et al. (2019). Finally, Section 3.5 outlines the expected cash flows of the proposed longevity bonds using the interest rate and systematic mortality model simulations and discusses the pricing of the bonds including the mortality assumption allowing for potential adverse selection arising from then mortality used to price the different types of individual longevity bonds.

3.1 Age and Cohort Assumptions

To illustrate the pricing and hedging of the individual longevity bonds we make the following assumptions. The proposed longevity bonds are issued to Australian males aged 65 on 01/01/2019, targeting the cohort born in 1954. The maximum attainable age is assumed to be 110. The modeling time period is therefore from the start of year 2019 to the end of year 2064.

3.2 Affine Model Framework

The affine model assumes that the term structure of interest rates and the age-cohort mortality rates are driven by level, slope and curvature risk factors, or state variables. The factors, or state variables, are $X_t = (L_t, S_t, C_t)^\top$, where L_t is the level factor, S_t the slope factor, and C_t the curvature factor, and are assumed to follow stochastic differential equations (SDE) under the risk neutral measure $\mathbb{Q}$:

$$\mathrm{d}X_t = K^{\mathrm{Q}} \left[\theta^{\mathrm{Q}}(t) - X_t\right] \mathrm{d}t + \Sigma(t)\, \mathrm{d}W_t^{\mathrm{Q}}, \tag{1}$$

where K^{Q} is a 3×3 matrix, the drift term $\theta^{\mathrm{Q}}(t)$ is a 3×1 vector, W_t^{Q} is a vector of 3 independent Brownian motions under the risk-neutral measure $\mathbb{Q}$, and $\Sigma(t)$ is a 3×3 variance-covariance matrix.

The instantaneous interest rate, or mortality rate, is given by an affine form:

$$r(t) = \rho_0(t) + \rho_1(t)^\top X_t,$$

where $\rho_0(t)$ and $\rho_1(t)$ are 3×1 vectors of continuous bounded functions.

Using an arbitrage-free requirement under the risk-neutral measure, the discount factor $D\,(t,T)$ for interest rates, or zero-coupon bond price, is given by (Christensen et al., 2011):

$$D\,(t,T) = \mathbb{E}^Q \left[e^{-\int_t^T r(u)\,\mathrm{d}u}\right] = e^{B(t,T)^\top X_t + A(t,T)},$$

where $D\,(t,T)$ is the time t price of a zero-coupon bond that matures at time T, and $B(t,T)$ and $A(t,T)$, the factor loadings, are solutions to the following system of ordinary differential equations (ODEs) (Duffie and Kan, 1996):

$$\begin{aligned} \frac{\mathrm{d}B(t,T)}{\mathrm{d}t} &= \rho_1(t) + \left(K^Q\right)^\top B(t,T), \\ \frac{\mathrm{d}A(t,T)}{\mathrm{d}t} &= \rho_0(t) - B(t,T)^\top K^Q \theta^Q - \frac{1}{2}\sum_{j=1}^{n} \left(\Sigma^\top B(t,T) B(t,T)^\top \Sigma\right)_{j,j}, \end{aligned} \tag{2}$$

with boundary conditions of $B(T,T) = 0$ and $A(T,T) = 0$. In the case of the age-cohort mortality rates, the discount factors are risk-adjusted survival probabilities.

3.2.1 Change of Measure

Girsanov's theorem is applied, as in Christensen et al. (2011), to change from the risk-neutral probability measure $\mathbb{Q}$ to the real-world probability measure $\mathbb{P}$:

$$\mathrm{d}W_t^Q = \mathrm{d}W_t^P + \Lambda_t\, \mathrm{d}t, \quad \Lambda_t = \lambda^0 + \lambda^1 X_t, \tag{3}$$

where Λ_t represents the market price of risk, λ^0 is a 3×1 vector and λ^1 is a 3×3 matrix.

The state variables under the real-world probability measure $\mathbb{P}$ are driven by the differential

equations:

$$\begin{aligned}
\mathrm{d}X_t &= K^{\mathrm{Q}}\left[\theta^{\mathrm{Q}} - X_t\right]\mathrm{d}t + \Sigma(\mathrm{d}W_t^{\mathrm{Q}} + \Lambda_t\,\mathrm{d}t) \\
&= K^{\mathrm{Q}}\left[\theta^{\mathrm{Q}} - X_t\right]\mathrm{d}t + \Sigma(\mathrm{d}W_t^{\mathrm{Q}} + (\lambda^0 + \lambda^1 X_t)\,\mathrm{d}t) \\
&= (K^Q - \Sigma\lambda^1)\left[\frac{K^Q\theta^Q + \Sigma\lambda^0}{K^Q} - X_t\right]\mathrm{d}t + \Sigma\,\mathrm{d}W_t^{\mathrm{P}} \\
&= K^{\mathrm{P}}\left[\theta^{\mathrm{P}} - X_t\right]\mathrm{d}t + \Sigma\,\mathrm{d}W_t^{\mathrm{P}}, \qquad (4)
\end{aligned}$$

where

$$K^P = K^Q - \Sigma\lambda^1, \quad \theta^P = \frac{K^Q\theta^Q + \Sigma\lambda^0}{K^Q}.$$

3.2.2 Parameter Estimation

Maximum likelihood using the Kalman filter is used for parameter estimation. The parameter vector is ψ, which are the parameters for the dynamics of the model. This requires a state transition equation and a measurement equation. The state transition equation gives the relationship for the state variables vector X between time t and $t-1$ and is a discrete time version of the state transition SDE's under the $\mathbb{P}$ measure:

$$X_t = \Phi_t^{X,0}(\psi) + \Phi_t^{X,1}(\psi)X_{t-1} + \eta_t,$$

where $\Phi_t^{X,0}(\psi) = (I - \exp\left(-K^P\Delta t\right))\theta^P$, $\Phi_t^{X,1}(\psi) = \exp\left(-K^P\Delta t\right)$, $\Delta t = 1$ represents the time step which depends on the time interval for the data used, and η_t is the error term.

The measurement equation gives the relationship between vector of yields to maturity y_t, or age-cohort mortality rates, at time t, in terms of the state variables as:

$$y_t = A + BX_t + \varepsilon_t,$$

where $A = -A(t,T)/(T-t)$ and $B = -B(t,T)/(T-t)$.

The error terms in state transition and measurement equations are assumed to be independent and follow normal distributions with zero means:

$$\begin{pmatrix} \eta_t \\ \varepsilon_t \end{pmatrix} \sim N\left[\begin{pmatrix} 0 \\ 0 \end{pmatrix}, \begin{pmatrix} Q & 0 \\ 0 & H \end{pmatrix}\right].$$

where the covariance matrix Q of the transition errors and covariance matrix H of the measurement errors are assumed diagonal with standard deviations σ_η and σ_ε respectively. The form of these standard deviations for the interest rate and mortality models are specified later.

A Kalman filter is used to estimate the parameters with an iterative process, beginning with initial estimates of X_0 and Σ_0, applying the following steps to update with the empirical data for the yields and mortality rates for each time step:

Step 1. Take the initial estimates of X_{t-1} and Σ_{t-1} from the previous iteration.

Step 2. Predict the values of X_t and Σ_t using yield to maturity and survival probability

information up to time $t-1$:

$$X_{t|t-1} = \mathbb{E}\left[X_t|Y_{t-1}\right] = \Phi_t^{X,0}(\psi) + \Phi_t^{X,1}(\psi)X_{t-1},$$
$$\Sigma_{t|t-1} = \Phi_t^{X,1}(\psi)\Sigma_{t-1}\Phi_t^{X,1}(\psi)^\top + Q_t(\psi).$$

Step 3. Use the information y_t at time t to update forecasts of X_t and Σ_t:

$$X_t = \mathbb{E}\left[X_t|Y_t\right] = X_{t|t-1} + \Sigma_{t|t-1}B(\psi)^\top F_t^{-1}v_t,$$
$$\Sigma_t = \Sigma_{t|t-1} - \Sigma_{t|t-1}B(\psi)^\top F_t^{-1}B(\psi)\Sigma_{t|t-1},$$

where

$$v_t = y_t - \mathbb{E}\left[y_t|Y_{t-1}\right] = y_t - A(\psi) - B(\psi)X_{t|t-1},$$
$$F_t = \mathrm{cov}\left(v_t\right) = B(\psi)\Sigma_{t|t-1}B(\psi)^\top + H(\psi).$$

Step 4. Repeat Steps 1-3 recursively until the latest yields to maturity and survival probability information y_T is included.

Once the data is processed with the Kalman filter, the optimal parameter set ψ is determined as the one that maximizes the log-likelihood function based on the data:

$$\log l\left(y_1, \ldots, y_T; \psi\right) = \sum_{t=1}^{T}\left(-\frac{N}{2}\log(2\pi) - \frac{1}{2}\log\left(|F_t|\right) - \frac{1}{2}v_t^\top F_t^{-1}v_t\right).$$

3.3 AFNS Interest Rate Model

The interest rate model used is the independent AFNS interest rate model with the SDE under $\mathbb{Q}$ in matrix form given as:

$$\begin{pmatrix} \mathrm{d}L_t \\ \mathrm{d}S_t \\ \mathrm{d}C_t \end{pmatrix} = \begin{pmatrix} 0 & 0 & 0 \\ 0 & \delta & -\delta \\ 0 & 0 & \delta \end{pmatrix}\left[\begin{pmatrix} \theta_1^Q \\ \theta_2^Q \\ \theta_3^Q \end{pmatrix} - \begin{pmatrix} L_t \\ S_t \\ C_t \end{pmatrix}\right]\mathrm{d}t + \begin{pmatrix} \sigma_{11} & 0 & 0 \\ 0 & \sigma_{22} & 0 \\ 0 & 0 & \sigma_{33} \end{pmatrix}\begin{pmatrix} \mathrm{d}W_t^{L,Q} \\ \mathrm{d}W_t^{S,Q} \\ \mathrm{d}W_t^{C,Q} \end{pmatrix},$$

where L_t, S_t and C_t represent the level, slope and curvature factors respectively. Here δ is a decay factor in K^{Q} that is required to match the Nelsen-Siegel model factor loadings. Although the θ_1^Q, θ_2^Q and θ_3^Q are set to zero in the implementation, the mean-reverting structure is shown in this equation for completeness.

The matrix representation of the SDE under the $\mathbb{P}$ measure is:

$$\begin{pmatrix} \mathrm{d}L_t \\ \mathrm{d}S_t \\ \mathrm{d}C_t \end{pmatrix} = \begin{pmatrix} k_{11}^P & 0 & 0 \\ 0 & k_{22}^P & 0 \\ 0 & 0 & k_{33}^P \end{pmatrix}\left[\begin{pmatrix} \theta_1^P \\ \theta_2^P \\ \theta_3^P \end{pmatrix} - \begin{pmatrix} L_t \\ S_t \\ C_t \end{pmatrix}\right]\mathrm{d}t + \begin{pmatrix} \sigma_{11} & 0 & 0 \\ 0 & \sigma_{22} & 0 \\ 0 & 0 & \sigma_{33} \end{pmatrix}\begin{pmatrix} \mathrm{d}W_t^{L,P} \\ \mathrm{d}W_t^{S,P} \\ \mathrm{d}W_t^{C,P} \end{pmatrix},$$

where k_{11}^P, k_{22}^P, k_{33}^P are the parameters that control the speed of mean-reversion to the long-term mean θ_1^P, θ_2^P, θ_3^P of the level, slope and curvature factors.

Under the AFNS structure, to ensure the zero-coupon bond price has the required factor loading structure, the short rate is $r(t) = L_t + S_t$. This means that $\rho_0(t) = \begin{pmatrix} 0 \\ 0 \\ 0 \end{pmatrix}$ and $\rho_1(t) = \begin{pmatrix} 1 \\ 1 \\ 0 \end{pmatrix}$

in the affine short rate equation $r(t) = \rho_0(t) + \rho_1(t)^\top X_t$.

For the above model, solving the ODEs in Equations (2) gives the AFNS factor loadings below:

$$B^1(t,T) = -(T-t), \quad B^2(t,T) = -\frac{1-e^{-\delta(T-t)}}{\delta}, \quad B^3(t,T) = (T-t)e^{-\delta(T-t)} - \frac{1-e^{-\delta(T-t)}}{\delta},$$
$$A(t,T) = \frac{1}{2}\int_t^T \sum_{j=1}^{3} \left(\Sigma^\top B(s,T)B(s,T)^\top \Sigma\right)_{j,j} \mathrm{d}s,$$

where $B(t,T)$ and $A(t,T)$ are dependent on the term to maturity $(T-t)$ but not the time.

Since $D(t,T) = e^{-(T-t)y(t,T)}$, where $y(t,T)$ stands for the yield to maturity of a zero-coupon bond between time t and T, we have:

$$y(t,T) = -\frac{1}{T-t}\log D(t,T) = -\frac{B(t,T)^\top}{T-t}X_t - \frac{A(t,T)}{T-t}.$$

Substituting $A(t,T)$ and $B(t,T)$, the AFNS model for the zero-coupon bond yield to maturity is:

$$y(t,T) = L_t + S_t\left(\frac{1-e^{-\delta(T-t)}}{\delta(T-t)}\right) + C_t\left(\frac{1-e^{-\delta(T-t)}}{\delta(T-t)} - e^{-\delta(T-t)}\right) - \frac{A(t,T)}{T-t}, \tag{5}$$

where the yield adjustment term $-\frac{A(t,T)}{T-t}$ is given by:

$$\begin{aligned}-\frac{A(t,T)}{T-t} =& -\sigma_{11}^2\frac{(T-t)^2}{6} - \sigma_{22}^2\left[\frac{1}{2\delta^2} - \frac{1}{\delta^3}\frac{1-\mathrm{e}^{-\delta(T-t)}}{T-t} + \frac{1}{4\delta^3}\frac{1-\mathrm{e}^{-2\delta(T-t)}}{T-t}\right] \\ & - \sigma_{33}^2\left[\frac{1}{2\delta^2} + \frac{1}{\delta^2}e^{-\delta(T-t)} - \frac{1}{4\delta}(T-t)e^{-2\delta(T-t)} - \frac{3}{4\delta^2}e^{-2\delta(T-t)}\right. \\ & \left. - \frac{2}{\delta^3}\frac{1-e^{-\delta(T-t)}}{T-t} + \frac{5}{8\delta^3}\frac{1-e^{-2\delta(T-t)}}{T-t}\right].\end{aligned}$$

3.3.1 Interest Rate Data

To estimate the AFNS interest rate model we use daily Australian zero-coupon bond yields from 1992 to 2018, obtained from the Reserve Bank of Australia. Figure 1 plots the Australian zero-coupon yield curves between the term to maturity of 0 to 10 years for the years 1992 to 2018.

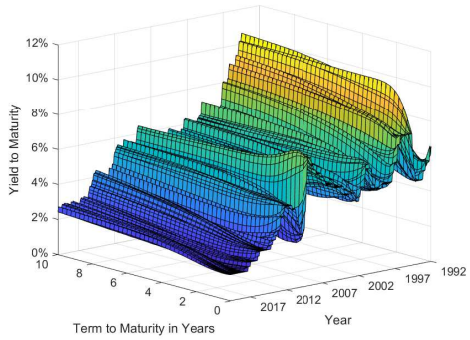

Figure 1: Yield to Maturity of Australian Zero Coupon Bonds from 1992 to 2018.

3.3.2 Interest Rate Model Estimation Results

Table 1: AFNS Interest Rate Model Estimated Parameters.

k_{11}^P	k_{22}^P	k_{33}^P	σ_{11}	σ_{22}	σ_{33}
0.00964	0.19603	1.77276	5.454e-03	9.994e-03	3.251e-02
θ_1^P	θ_2^P	θ_3^P	σ_ε	δ	
0.06625	-0.02005	-0.02060	5.586e-04	0.73174	

Table 1 shows the estimation results of the AFNS interest rate model. σ_ε is the standard deviation in the measurement equation. The estimated long-term mean θ_1^P, θ_2^P, and θ_3^P for level, slope and curvature are 6.63%, -2.01% and -2.06% respectively, so that the long-term mean for the long-term yield is 6.63%, and that of the short rate is 4.62%. k_{33}^P is larger than k_{11}^P and k_{22}^P, so that the curvature factor has the highest speed of mean-reversion, followed by the slope and then level factors. This reflects the longer time period for the impact of changes in the level of the yield curve as compared with the shorter term impact of changes in the curvature of the yield curve. The positive δ means the slope factor has a larger effect on the short rate, and the curvature factor has a larger effect on the medium-term rate, which can also be seen in Figure 4.

3.3.3 Interest Rate Model Goodness of Fit

The Root Mean Square Error (RMSE), the Akaike information criterion (AIC), and the Bayesian information criterion (BIC) of the fitted model are displayed in Table 2. RMSE is a scale-dependent measure of error, meaning that the RMSE of a particular variable can be compared between models, but not between variables (Hyndman and Koehler, 2006). The RMSE of 0.0005 for the fitted yields is comparable with the RMSE calculated with the yield data and parameters in Christensen et al. (2011) of 0.0017. The other measures like the log likelihood, AIC and BIC are not directly comparable to other models estimated with different data-sets.

Table 2: AFNS Interest Rate Model Goodness of Fit.

Log likelihood	RMSE	No. of parameters	No. of observations	AIC	BIC
1643526.14	0.0005	11	274536	-3287030.27	-3286914.52

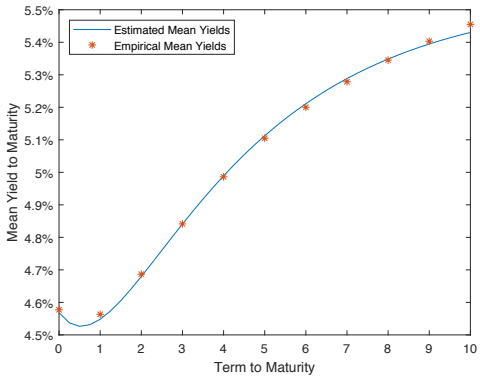

(a) Empirical and Estimated Mean Yield Curves.

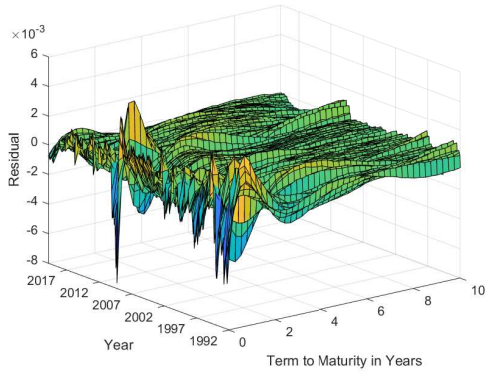

(b) Residuals of the Fitted AFNS Interest Rate Model.

Figure 2: AFNS Interest Rate Model Goodness of Fit to Australian Data, from 1992 to 2018.

Figure 2(a) compares the estimated mean yield curve to the empirical mean yields. The estimation and model fitting results show how the model estimated mean yield curve fits the empirical data well.

Figure 2(b) shows the residuals of the model. The residuals are generally lower than 2×10^{-3}, except for the short rates between 2007 and 2008. This exception is mainly due to the volatility of short rates during the global credit crisis.

To assess the performance of the model, we also simulate the three-month yield from December 2017 to December 2018 with a step size of a month, and compare the mean of the simulated three-month yield to the empirical three-month yield. Yield curves are readily simulated using the transition equation for their evolution over time, given by:

$$X^1_{t+\Delta t} = (1 - e^{-k^p_{11}\Delta t})\theta^P_1 + e^{-k^p_{11}\Delta t} X^1_t + \sqrt{\frac{\sigma^2_{11}}{2k^P_{11}}\left(1 - e^{-2k^p_{11}\Delta t}\right)}\mathcal{Z}^1_t,$$

$$X^2_{t+\Delta t} = (1 - e^{-k^p_{22}\Delta t})\theta^P_2 + e^{-k^p_{22}\Delta t} X^2_t + \sqrt{\frac{\sigma^2_{22}}{2k^P_{22}}\left(1 - e^{-2k^p_{22}\Delta t}\right)}\mathcal{Z}^2_t,$$

$$X^3_{t+\Delta t} = (1 - e^{-k^p_{33}\Delta t})\theta^P_3 + e^{-k^p_{33}\Delta t} X^3_t + \sqrt{\frac{\sigma^2_{33}}{2k^p_{33}}\left(1 - e^{-2k^p_{33}\Delta t}\right)}\mathcal{Z}^3_t,$$

where Δt is time step, and $\mathcal{Z}^1_t$, $\mathcal{Z}^2_t$, $\mathcal{Z}^3_t$ are three independent random variables that follow standard normal distributions.

We simulate 20,000 paths for each of the three factors.

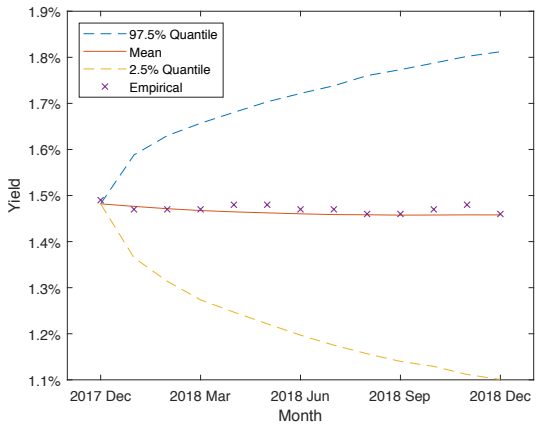

Figure 3: Simulated Three-Month Yield Compared With Empirical Three-Month Yield, from December 2017 to December 2018.

The comparison between empirical and model short rates is shown in Figure 3, with the 95% confidence interval. It is clear that there is a wide confidence interval reflecting the high volatility of the short term interest rates. The simulated three-month yields are seen to effectively capture the slight downward trend in the short rate between 2017 and 2018.

3.3.4 Interest Rate Model - Estimated Factors and Factor Loadings

The factor loadings and the yield adjustment term with the estimated parameters are shown in Figure 4. The factor loading for the level factor is a constant of 1, since it impacts all terms to maturity the same. The factor loading for the slope factor is decreasing over maturity, indicating how the slope factor influences the short-term yields more than the long term yields

hence changing the slope of the yield curve. The factor loading of the curvature factor is hump shaped, so that the curvature factor mainly affects the medium-term yields. The yield adjustment term, which is required to ensure the non-arbitrage constraint is met, is downward shaped as in Christensen et al. (2011).

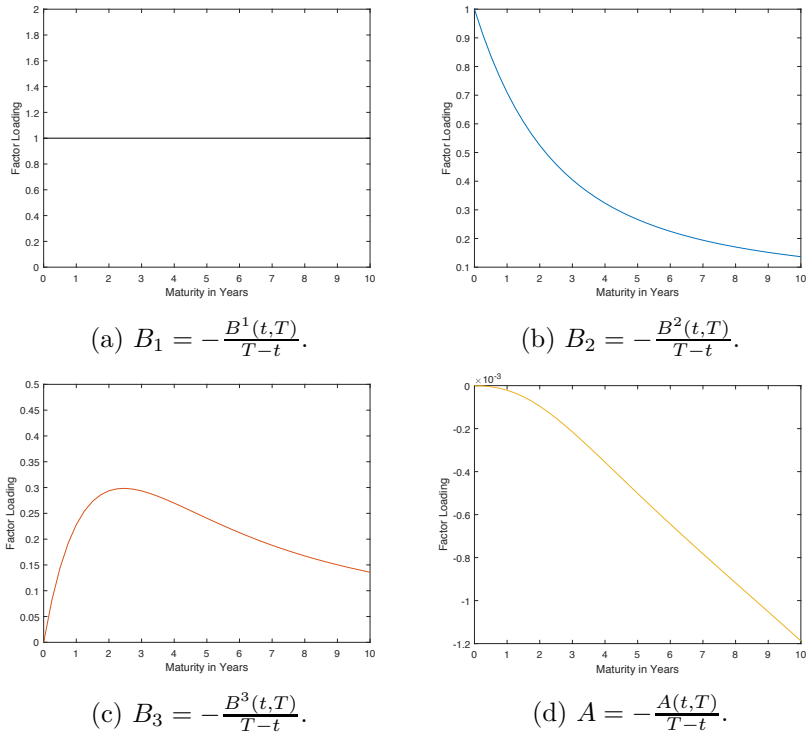

(a) $B_1 = -\frac{B^1(t,T)}{T-t}$. (b) $B_2 = -\frac{B^2(t,T)}{T-t}$.

(c) $B_3 = -\frac{B^3(t,T)}{T-t}$. (d) $A = -\frac{A(t,T)}{T-t}$.

Figure 4: Factor Loadings of the AFNS Interest Rate Model.

Figure 5 shows the evolution of the factors. The level factor is steadily decreasing after the Global Credit Crisis in 2008, indicating a structural change in the level of interest rate since that time. A negative slope factor indicates that the yield curve is upward shaped, while a positive slope factor indicates a downward sloped yield curve. The slope factor is found to be positive mainly between 2005 and 2008, reflecting the inverted yield curves during that period. The overall trend of the slope factor is increasing after 2009, and the yield curves have become flatter since then. The curvature factor is increasing after year 2012, capturing an increase in the curvature of the the yield curve since 2012.

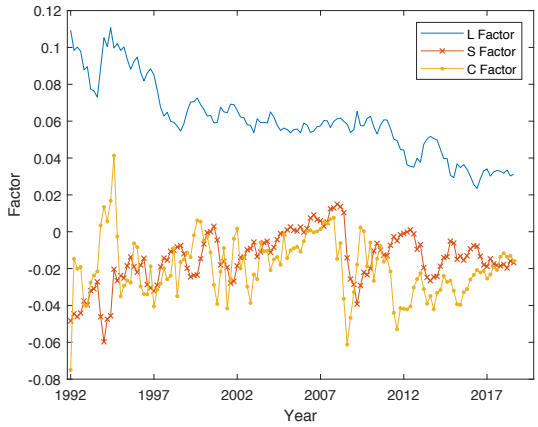

Figure 5: Factors of the AFNS Interest Rate Model, from 1992 to 2018.

3.3.5 Simulated One Month Interest Rates

The modeling period for the proposed longevity bond is from year 2019 to the end of year 2064 and the frequency of the payments is monthly. For the determination of surplus on the hedging portfolio and for the present valuation of the surplus we use the one-month yield. We simulate the one-month yield to maturity from the end of year 2018 to the end of year 2064, with a monthly simulation step of $\Delta t = 1/12$.

The simulation results are shown in Figure 6. The mean of the simulated one-month yield to maturity initially reduces for the first five years, then steadily increases to around 2% for the next 40 years. This reflects and captures the current low interest rate environment as well as the continuation of this into the future.

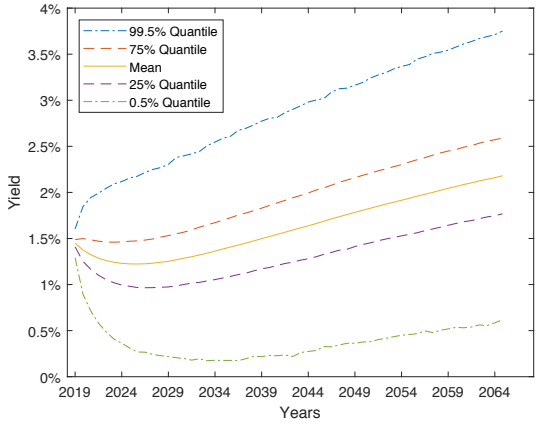

Figure 6: Mean One-Month Yield with the 25%, 75%, 0.5%, and 99.5% Quantiles.

3.4 AFNS Systematic Mortality Model

The dynamics for the mortality rates are also modeled with the independent AFNS model. Analogous to modeling the yield curve with yields to maturity for different terms to maturity, the AFNS mortality model uses the mortality rate curve with different average mortality rates for future ages of death. The average force of mortality $\overline{\mu}(t,T)$ between time t and T is given

by:

$$\overline{\mu}(t,T) = L_t + S_t\left(\frac{1-e^{-\delta_\mu(T-t)}}{\delta_\mu(T-t)}\right) + C_t\left(\frac{1-e^{-\delta_\mu(T-t)}}{\delta_\mu(T-t)} - e^{-\delta_\mu(T-t)}\right) - \frac{A(t,T)}{T-t}, \tag{6}$$

where δ_μ is the AFNS decay factor in the mortality model.

The survival probability of an individual aged x at t from t to T is (Blackburn and Sherris, 2013):

$$S(t,T,x) := \mathbb{E}^Q\left[e^{-\int_t^T \mu(s)\,\mathrm{d}s}\right] = e^{-(T-t)\overline{\mu}(t,T)},$$

where $\mu(t)$ stands for the mortality intensity of individual aged x at t. The notation age x in the survival probability $S(t,T)$ is dropped in the remainder of the paper, because x is fixed to be 65 as the lower bound of our interested age period.

We follow Blackburn and Sherris (2013) and set $\theta^{\mathrm{P}}(t)$ to 0. The state variable model under the $\mathbb{P}$ measure becomes:

$$\begin{pmatrix} \mathrm{d}L_t \\ \mathrm{d}S_t \\ \mathrm{d}C_t \end{pmatrix} = -\begin{pmatrix} k^P_{\mu,11} & 0 & 0 \\ 0 & k^P_{\mu,22} & 0 \\ 0 & 0 & k^P_{\mu,33} \end{pmatrix}\begin{pmatrix} L_t \\ S_t \\ C_t \end{pmatrix}\mathrm{d}t + \begin{pmatrix} s_{11} & 0 & 0 \\ 0 & s_{22} & 0 \\ 0 & 0 & s_{33} \end{pmatrix}\begin{pmatrix} \mathrm{d}W^{L,P}_t \\ \mathrm{d}W^{S,P}_t \\ \mathrm{d}W^{C,P}_t \end{pmatrix},$$

where s_{ii} $(i = 1,2,3)$ are the volatility parameters in the covariance matrix of the mortality model.

The AFNS model has the possibility of generating negative mortality rates since the mortality rate is normally distributed. However, it has been shown that the probability of negative mortality in the model is extremely small. This includes when the model is calibrated to Danish data (Xu et al., 2019) and to US data (Huang et al., 2019).

With θ^P equal to 0 in the AFNS mortality model, the transition equation is given by:

$$X_t = \exp\left(-K^P\right)X_{t-1} + \eta_t.$$

The measurement equation for the mortality model is:

$$\overline{\mu}_t = BX_t + A + \varepsilon_t,$$

where $\overline{\mu}_t$ is a 45×1 vector of the average force of mortality, $\overline{\mu}(t,T)$, for $T-t = 1$ to 45 at time t.

The error terms η_t and ε_t are assumed to follow the error structure:

$$\begin{pmatrix} \eta_t \\ \varepsilon_t \end{pmatrix} \sim N\left[\begin{pmatrix} 0 \\ 0 \end{pmatrix}, \begin{pmatrix} R & 0 \\ 0 & H \end{pmatrix}\right]$$

In the mortality model, to capture Poisson variation, the variance of the measurement error ε_t is assumed to be higher for larger $T-t$, and the covariance matrix H has the structure below:

$$H(t,T) = \frac{1}{T-t}\sum_{i=1}^{T-t}\left[r_c + r_1 e^{r_2 i}\right],$$

where r_1, r_2 and r_c are three parameters in the parameter set estimated using the Kalman filter.

3.4.1 Mortality Data

Age-cohort mortality data is used to estimate the AFNS mortality model which better captures the cohort mortality required to price the longevity bond as discussed in Huang et al. (2019). The cohort mortality data from ages 65 to 110 are extracted by taking the diagonal of the death rates q from the Australian life table data, where:

$$S(t,T) = \prod_{s=1}^{T-t} \left[1 - q(65+s-1, t+s-1)\right], \quad \bar{\mu}(t,T) = -\frac{1}{T-t} \log\left[S(t,T)\right],$$

where $S(t,T)$ is the survival probability from time t to T for the cohort aged 65 at time t, and $q(x,t)$ is the one-year probability of death for the cohort aged x at time t.

The age-cohort average force of Australian male mortality is shown in Figure 7. The 1856 to 1907 cohorts have full observations of all cohort mortality rates from age 65 to 110. A downward trend over time can be observed in Figure 7, capturing the mortality improvement in the age-cohort data.

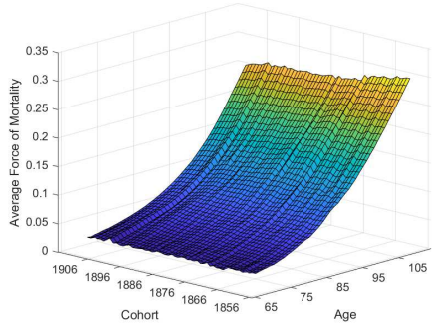

Figure 7: Australian Cohort Average Force of Mortality for Males Born between 1856 and 1907, from Age 65 to 110.

3.4.2 Mortality Model Estimation Results

Table 3: AFNS Mortality Model Estimated Parameters.

$k^P_{\mu,11}$	$k^P_{\mu,22}$	$k^P_{\mu,33}$	s_{11}	s_{22}	s_{33}
1.755e-01	5.871e-03	7.667e-03	1.041e-03	1.238e-04	4.357e-05
r_1	r_2	r_c	δ_μ		
1.183e-13	0.42060	2.042e-06	-0.10708		

Table 3 gives the estimated parameters of the AFNS mortality model. In contrast to the AFNS interest rate model, the estimated δ_μ in the mortality model is negative, consistent with the parameter estimates of the AFNS mortality models in Blackburn and Sherris (2013); Xu et al. (2019); Huang et al. (2019). Larger parameter values for k^P_μ mean that the factor is mean-reverting to zero, whereas for values of k^P_μ close to zero this means that the factor is closer to a random walk (Blackburn and Sherris, 2013). The values for the Poisson variation given by r_1, r_2 and r_c are consistent with Blackburn and Sherris (2013), which captures an exponential increase expected in the measurement error with age.

3.4.3 Systematic Mortality Model Goodness of Fit

Table 4: AFNS Mortality Model Goodness of Fit.

Log likelihood	RMSE	No. of parameters	No. of observations	AIC	BIC
-10840.63	0.0016	10	2340	-21661.26	-21603.69

Table 4 shows the log likelihood, RMSE, AIC and BIC to assess the goodness of fit of the AFNS mortality model. The RMSE of the estimated independent AFNS mortality model is 0.0016, as compared to 0.0012 in Blackburn and Sherris (2013) and 0.0007 in Huang et al. (2019) for different datasets. The RMSE is slightly higher than the model calibrated to the Swedish or the US mortality data reflecting a higher volatility in the Australian cohort data.

Figure 8(a) displays the mean absolute percentage error (MAPE) of the fitted survival curves across cohorts from age 65 to 110. The MAPE of the model is compared with Huang et al. (2019) which is calibrated to the US male cohort mortality data, and the results show a similar pattern and increase with age. The MAPE for the survival curve is below 6% up to age 100. For ages above 100, a small absolute error in the survival probability leads to a relatively large percentage error at these ages. The MAPE also demonstrates that the independent AFNS mortality model is an adequate fit to the Australian cohort mortality data.

Figure 8(b) shows the absolute residuals of the fitted AFNS mortality model. Most of the errors are below 5×10^{-3}, and the residuals are evenly distributed with no significant trend observed, confirming that the model is a good fit to the Australian data.

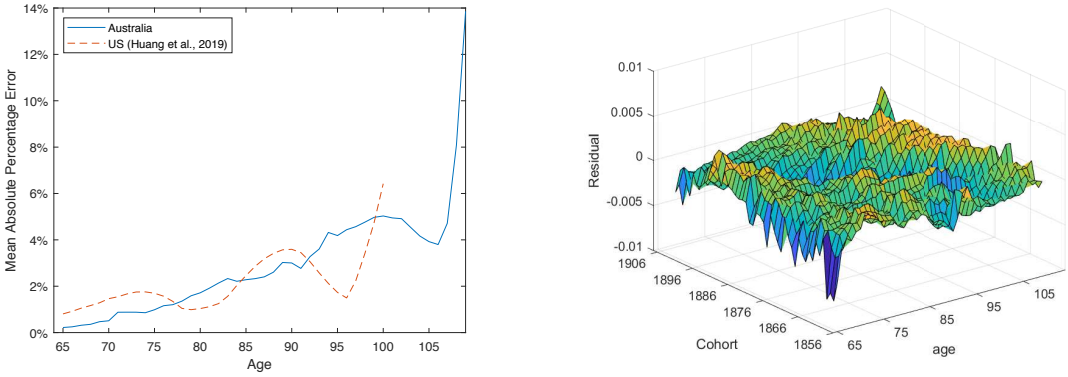

(a) MAPE of the Survival Probabilities Compared with US Model.

(b) Residuals of the AFNS Mortality Model.

Figure 8: AFNS Mortality Model Goodness of Fit to Australian Mortality Data.

3.4.4 Systematic Mortality Model - Estimated Factors and Factor Loadings

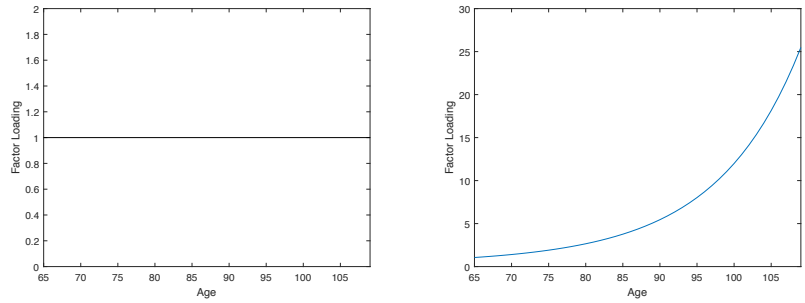

(a) $B_1 = -\frac{B^1(t,T)}{T-t}$.

(b) $B_2 = -\frac{B^2(t,T)}{T-t}$.

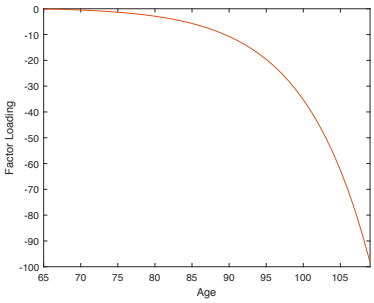

(c) $B_3 = -\frac{B^3(t,T)}{T-t}$.

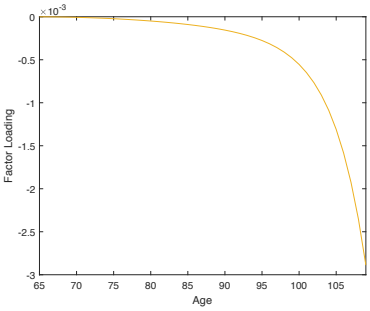

(d) $A = -\frac{A(t,T)}{T-t}$.

Figure 9: Factor Loadings of the AFNS Mortality Model.

The factor loadings with the estimated parameters are shown in Figure 9. The loading for the level factor is constant at 1, since the level factor affects all ages equally. Because of the negative δ_μ shown in Table 3, the factor loading for the slope factor is exponentially increasing from 1 to 25, and the factor loading for the curvature factor is exponentially decreasing from 0 to -100. The scale of the third factor loading is larger than the first two, so that the third factor mainly captures the mortality changes at older ages.

The evolution of the level, slope and curvature factors from 1922 to 1972 are shown in Figure 10. These are for the age-cohort mortality curves. They show the year that the cohort was aged 65 years old. All three factors were relatively constant for the mortality curve of 65 year old individuals before year 1935. After 1935, the slope factor decreases at an increasing rate, while the level factor steadily increases. Since the loading for the slope factor increases exponentially compared to the constant B_1 equal to 1, these jointly capture the mortality improvement pattern in the age-cohort mortality curves after 1935. The curvature factor is much smaller and is decreasing over time. The large reduction in the slope factor and slight reduction in the curvature factor allows the model to capture the reduction of the average force of mortality at older ages.

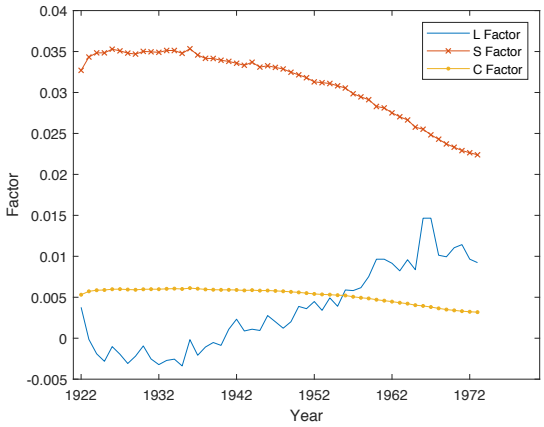

Figure 10: Factors of the AFNS Mortality Model, from 1922 to 1972.

3.4.5 Forecasting Cohort Survival Curves

The model is fitted using the cohorts with year of birth between 1856 and 1907. Our analysis is for bonds issued to the 1954 cohort, so that a best estimate is required for the expected survival curve for the 1954 cohort. The optimal forecast methodology for yield curves is given in Christensen et al. (2011). We adapt this methodology to forecast the best estimate mortality curve, using:

$$E\left[L_{t+\Delta t}|L_t\right] = e^{-k^P_{\mu,11}\Delta t}L_t, \quad E\left[L^2_{t+\Delta t}|S_t\right] = e^{-k^P_{\mu,22}\Delta t}S_t, \quad E\left[S_{t+\Delta t}|S_t\right] = e^{-k^P_{\mu,33}\Delta t}S_t,$$
$$\overline{\mu}_{t+\Delta t} = B^\top \times E\left[X_{t+\Delta t}|X_t\right] + A.$$

To demonstrate the performance of this method for the age-cohort mortality curves we use to derive the best estimate, we compare the empirical survival probabilities of the 1907 cohort with the best estimate survival probabilities for the 1907 cohort derived from the 1906 cohort, 1905 cohort and 1897 cohort, projecting $i = 1, 2, 10$ years ahead.

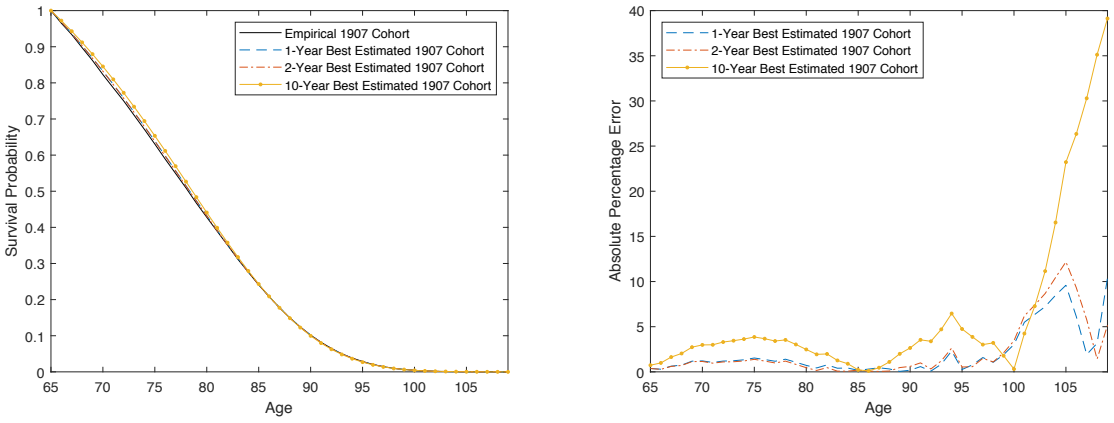

(a) Empirical and Best Estimated Survival Probabilities.

(b) Absolute Percentage Errors of Best Estimated Survival Probabilities.

Figure 11: Empirical and Best Estimated Survival Probabilities and Absolute Percentage Errors.

Figure 11(a) shows the comparison of the empirical survival curve of the 1907 cohort with the

best estimate survival curves. The best estimate survival curves show a good fit compared to the empirical survival curve. Figure 11(b) shows the absolute percentage errors of the best estimate survival curves. All three curves have low absolute percentage error up to age 100. The higher absolute percentage error after age 100 reflects the low survival probabilities at these older ages which approach 0 after age 100. Below age 100, the error of the one year and two year forecasts are always below 3%. The 10-year forecast has a slightly higher absolute error, although most of the errors are below 5%. These demonstrate that the fitted mortality model and the best estimate forecasts are accurate and well suited for our application with a good fit to historical cohort survival curves and low levels of forecast error.

3.4.6 Simulation of Survival Curves

To assess the effectiveness of the government bond immunizing portfolio, and to quantify capital requirements and loadings, we need to generate a surplus distribution for the special purpose vehicle. To do this we require to generate a distribution for the survival probabilities. To do this we use the transition equation to simulate 20,000 paths for the 1954 cohort survival probabilities using the best-estimate factors.

With θ^P set to zero, and the forecast horizon Δt of 1, the transition equation of the mortality model is:

$$L_{t+1} = e^{-k^p_{\mu,11}} L_t + \sqrt{\frac{s^2_{11}}{2k^P_{\mu,11}}\left(1 - e^{-2k^p_{\mu,11}}\right)}\mathcal{Z}^1_t, \quad S_{t+1} = e^{-k^p_{\mu,22}} S_t + \sqrt{\frac{s^2_{22}}{2k^P_{\mu,22}}\left(1 - e^{-2k^p_{\mu,22}}\right)}\mathcal{Z}^2_t,$$

$$C_{t+1} = e^{-k^p_{\mu,33}} C_t + \sqrt{\frac{s^2_{33}}{2k^p_{\mu,33}}\left(1 - e^{-2k^p_{\mu,33}}\right)}\mathcal{Z}^3_t,$$

where $\mathcal{Z}^1_t$, $\mathcal{Z}^2_t$, and $\mathcal{Z}^3_t$ are three independent random variables that following standard normal distributions. As time increases, the 1954 cohort ages, so the 1-year simulated survival probability after t years is:

$$S^j(t,t+1) = S^j_{1954+t}(t,t+1) = \frac{S^j_{1954+t}(0,t+1)}{S^j_{1954+t}(0,t)} = \frac{\exp\left(B(0,t+1)^\top \times X^j_{1954+t} + A(0,t+1)\right)}{\exp\left(B(0,t)^\top \times X^j_{1954+t} + A(0,t)\right)},$$

where $S^j_{1954+t}(0,t)$ is the t-year ahead simulated survival probability from age 65 to $65+t$, and j indicates the j^{th} path of the 20,000 simulations.

The 1-year simulated survival probabilities after t years are used to generate path of the simulated survival probabilities for the 1954 cohort using.

$$S^j(0,n) = \prod_{t=0}^{n-1} S^j(t,t+1), \quad \overline{\mu^j}(0,n) = -\frac{\log(S^j(0,n))}{n}.$$

Figure 12 shows the simulated force of mortality with 50% and 99% confidence intervals.

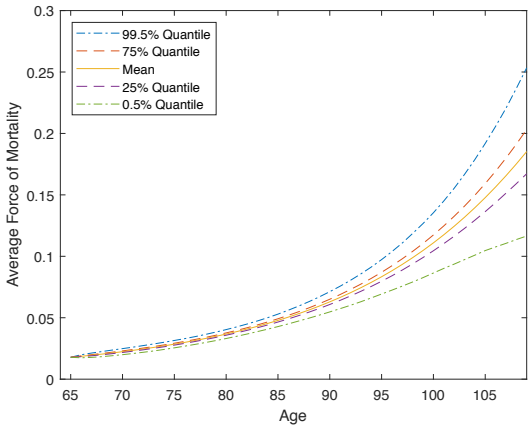

Figure 12: Mean Average Force of Mortality with the 25%, 75%, 0.5%, and 99.5% Quantiles.

From Figure 12 we see how the volatility increases with age, reflecting the higher uncertainty in the forecast as time increases and the cohort ages. Although the AFNS mortality model does not guarantee a positive force of mortality, Figure 12 shows that the 0.5% quantile of the force of mortality is above 0, so that negative mortality probabilities have low probability of occurring.

Figure 13 shows the mean of the simulated mortality curve and survival curve for the 1954 cohort compared with the empirical data for the 1907 cohort. Both Figure 13(a) and Figure 13(b) show a significant mortality improvement of the 1954 cohort compared to the 1907 cohort.

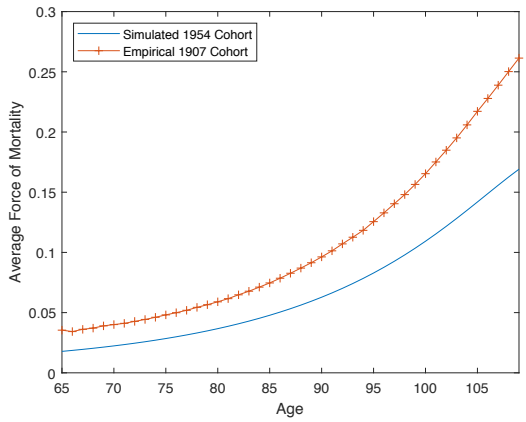

(a) Simulated 1954 Cohort Mortality Curve and Empirical 1907 Mortality Curve.

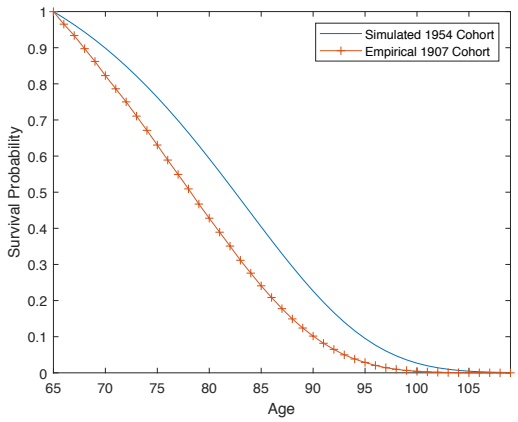

(b) Simulated 1954 Cohort Survival Probability and Empirical 1907 Survival Probability.

Figure 13: Simulation of the 1954 Cohort.

3.5 Pricing and Expected Cash Flows of Longevity Bonds

We use the calibrated systematic mortality model along with the interest rate model to quantify the impact of systematic mortality risk in determining the immunizing bond portfolio and quantifying the loading in the bond for systematic mortality risk. The LCP Bond has built in natural hedging from the income benefits and the death benefit which we assess when considering the capital loadings required for systematic mortality risk.

In pricing the individual bonds, some allowance for potential adverse selection in the mortality

assumption will be required in practice. The LCP Bond, if priced with an aggregate population mortality assumption, will be more attractive to individuals with higher self assessed mortality and the LAI Bond more attractive to individuals with lower self assessed mortality. The mortality rates in the mortality model would be increased for the LCP Bond and reduced for LAI Bond to allow for this.

The issuer of the longevity bonds aggregates the risks to produce monthly expected cash outflows. As a portfolio, the expected cash flow of the longevity bond at time t ($t = \frac{1}{12}, \frac{2}{12}, \frac{3}{12}, ...$) is given by:

$$ECF_t^\ell = \mathcal{S}^\ell \times S(0,t) + \mathcal{D}^\ell \times \left(S(0, t - \frac{1}{12}) - S(0,t) \right).$$

The price EPV^ℓ of the longevity bond ℓ is the sum of the expected present values of all the expected cash flows ECF^ℓ. This is given by

$$EPV^\ell = \mathcal{S}^\ell \cdot \sum_{u=1}^{\infty} D\left(0, \frac{u}{12}\right) \cdot S\left(0, \frac{u}{12}\right) + \mathcal{D}^\ell \cdot \sum_{u=1}^{\infty} D\left(0, \frac{u}{12}\right) \cdot \left(S\left(0, \frac{u-1}{12}\right) - S\left(0, \frac{u}{12}\right) \right).$$

Table 5 shows the survival benefit $\mathcal{S}^\ell$ and death benefit $\mathcal{D}^\ell$ of the two bonds that produce a standardized price of 100 using the population level age-cohort mortality model. The coupon cash flows are relatively small for the LCP Bond and they constitute 27.62% of the value of the bond. The flexible bonds have a weighted mix of these benefits reflecting the weights that an individual selects to reflect their preferences for bequest wealth.

Table 5: Survival and Death Benefits of $100 Price Standardized LCP Bond and LAI Bond.

	$\mathcal{S}$	$\mathcal{D}$	EPV	$EPV_{\mathcal{S}}/EPV$
LCP	0.15	91.03	100	27.62%
LAI	0.55	0.00	100	100%

The annualized expected cash flows of LCP Bond and LAI Bond are displayed in Figure 14. Since the LAI Bond only has a survival benefit, the expected payments steadily decrease over time, corresponding to the gradually decreasing survival curve. By contrast, the LCP Bond has both a coupon income survival benefit and a principal death benefit, so the expected cash flows first increase due to increasing number of expected deaths, then gradually reduces as the expected survivors reduce.

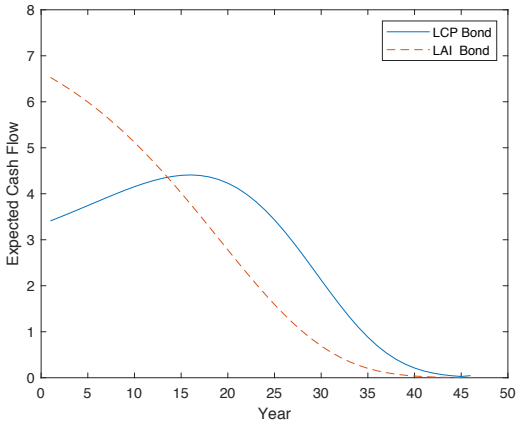

Figure 14: Expected Cash Flows of LCP Bond and LAI Bond, Both Standardized to Price = 100.

4 Optimally Immunized Bond Portfolios

The special purpose vehicle that issues the longevity bonds aggregates the expected cash flows on the bonds and then manages the risk of its liability portfolio by investing the proceeds of the bonds in an Australian government bond portfolio. This bond portfolio is selected to optimally immunize the interest rate risk and longevity risk. Since there are no traded longevity bonds in Australia, we construct the hedging portfolio from bonds available on the Australian market, including government coupon bonds and semi-government annuity bonds offered by the New South Wales (NSW) government.

Fundamental to the pricing and financial engineering of the individual longevity bonds is the risk management of the special purpose vehicle. This relies not only on the use of financial engineering models for interest rate and mortality developed and suited for financial applications such as the pricing of LCP and LAI individual longevity bonds, but also an effective immunization hedging strategy.

We present the method used for immunization of the individual longevity bonds, the details of the government bonds used and the immunization portfolios for the individual longevity bonds. We do this for the LCP and LAI Bonds since the flexible bonds are a weighted combination of these bonds. To show the effectiveness of the immunization strategy we measure the hedging performance by considering the expected cash flow match and the simulated distribution of the final year accumulated net cash flow portfolio surplus.

4.1 Immunization Strategy

Immunization is based on the duration and convexity of assets and liabilities. The Fisher-Weil dollar duration Dur and convexity Cov of longevity-linked securities are (Liu and Sherris, 2017):

$$Dur = \sum_{t \geq 0} ECF_t \cdot t \cdot D(0,t), \quad Cov = \sum_{t \geq 0} ECF_t \cdot t^2 \cdot D(0,t),$$

where ECF_t stands for the expected cash flow of the security at time t and $D(0,t)$ is the discount factor. The Fisher-Weil duration $\widetilde{\mathbf{D}}$ and convexity $\widetilde{\mathbf{C}}$ are defined as:

$$\widetilde{\mathbf{D}} = \frac{Dur}{EPV}, \quad \widetilde{\mathbf{C}} = \frac{Cov}{EPV}.$$

We follow Panjer et al. (1998); Liu and Sherris (2017) and use linear programming with a mean-absolute deviation constraint in order to optimally match the asset and liability expected cash flows. The immunization strategy is to select the optimal bond portfolio by minimizing the convexity of the asset-liability portfolio. Since the dollar convexity of the net asset-liability portfolio is negative, we maximize the negative dollar convexity, which is equivalent to minimizing the absolute value of the dollar convexity. The optimal portfolio is constrained to match the duration of the asset and liability expected cash flows, to match the expected present value of assets and liabilities and to satisfy a a mean-absolute deviation constraint. The immunization algorithm works with the Net Portfolio (NP) = Asset - Liability expected cash flows and values. The algorithm is as follows:

$$\max_{\mathbf{w}}(Cov_{NP}) \tag{7}$$

subject to:

$$Dur_{NP} = 0, \tag{8}$$

$$EPV_{NP} = \sum_t n_t = 0, \tag{9}$$

$$\sum_{t>0} n_t \times (t-h)^+ \leq 0 \text{ for all positive } h, \tag{10}$$

where

$$n_t = \sum_i w_i \times ECF_{i,t} \times D(0,t) - ECF_{LB,t} \times D(0,t)$$

w is a vector of bond weights where w_i giving the optimal bond portfolio weights for bond i with expected cash flow $ECF_{i,t}$ at time t, and $ECF_{LB,t}$ is the expected cash flow of the longevity bond at time t.

4.2 Bond Details

4.2.1 Individual Longevity Bonds

We determine immunized bond portfolios for the lifetime coupon and principal bond (LCP Bond) and the lifetime annuity income bond (LAI Bond). Other individual longevity bonds issued are a weighted combination of these two bonds so that optimal immunized bond portfolios are just a weighted combination of the results for these two bonds. The individual longevity bonds are standardized to the price of 100, so the weighting of bond i in the immunized bond portfolio for the Flexible LIPB Series $W\%$ is given as a weighted average of the lifetime coupon and principal bond (LCP Bond) and the lifetime annuity income bond (LAI Bond) using:

$$w_i^W = W\% \times w_i^{\text{LCP}} + (1 - W\%) \times w_i^{\text{LAI}}.$$

The bond details are listed in Table 6.

Both bonds are issued to an Australian male aged 65 on 01/01/2019 and have a monthly payment frequency (Freq = 12). The term to maturity (TTM) of $\omega - 65$ in Table 6 indicates a lifetime payment. The price of the bonds are standardized to 100 at the time of issue. The duration and convexity of the LCP Bond are higher than the LAI Bond, reflecting the fact that the LCP Bond has higher interest rate risk than the LAI Bond. The higher duration of LCP Bond is expected and can be seen from the higher expected cash flows at later ages as shown in Figure 14.

Table 6: Details of LCPB and LAIB.

Code	**Maturity**	**TTM**	**Freq**	**Price**	*Dur*	*Cov*	$\widetilde{\mathbf{D}}$	$\widetilde{\mathbf{C}}$
LCPB	ω	$\omega - 65$	12	100	1469.75	29843.77	14.70	298.44
LAIB	ω	$\omega - 65$	12	100	1036.66	16581.68	10.37	165.82

4.2.2 Bonds Used to Construct the Immunized Asset Portfolio

We include both coupon bonds and annuity bonds issued by governments in Australia in the immunization. The coupon bonds pay fixed coupon payments with face value API at maturity. The annuity bonds pay equal payments the term of the bond. Details of these bonds are presented, including payment amount and frequency, bond prices, the Fisher-Weil dollar duration

and convexity, and the Fisher-Weil duration and convexity.

Table 7 displays the details of the coupon bonds. These coupon bonds are exchanged-traded Treasury Bonds (eTBs) issued by the Australian government. The eTBs pay fixed semi-annual coupon payments and the a face value of 100 at maturity. The bonds have terms to maturity from 0.8 to 28.24 years, with the largest dollar duration of 2874.11, and largest dollar convexity of 72730.63, exceeding that of the two individual longevity bonds.

Table 7: Details of Australian Government Coupon Bonds.

Code	**Coupon**	**Maturity**	**TTM**	**FV**	**Freq**	**Price**	*Dur*	*Cov*	$\widetilde{\mathbf{D}}$	$\widetilde{\mathbf{C}}$
GSBS19	2.75%	21/10/2019	0.80	100	2	101.56	83.95	69.73	0.83	0.69
GSBG20	4.50%	15/04/2020	1.29	100	2	104.83	136.42	180.22	1.30	1.72
GSBU20	1.75%	21/11/2020	1.89	100	2	100.74	198.66	395.18	1.97	3.92
GSBI21	5.75%	15/05/2021	2.37	100	2	110.87	253.73	600.23	2.29	5.41
GSBW21	2.00%	21/12/2021	2.97	100	2	101.80	306.27	935.38	3.01	9.19
GSBM22	5.75%	15/07/2022	3.54	100	2	117.68	390.41	1386.98	3.32	11.79
GSBU22	2.25%	21/11/2022	3.89	100	2	103.58	398.62	1572.06	3.85	15.18
GSBG23	5.50%	21/04/2023	4.30	100	2	118.33	473.26	2016.05	4.00	17.04
GSBG24	2.75%	21/04/2024	5.31	100	2	107.76	546.39	2891.09	5.07	26.83
GSBG25	3.25%	21/04/2025	6.31	100	2	112.28	658.37	4090.05	5.86	36.43
GSBG26	4.25%	21/04/2026	7.31	100	2	121.25	790.72	5593.49	6.52	46.13
GSBG27	4.75%	21/04/2027	8.31	100	2	127.89	927.96	7435.60	7.26	58.14
GSBU27	2.75%	21/11/2027	8.89	100	2	112.38	917.91	8019.37	8.17	71.36
GSBI28	2.25%	21/05/2028	9.39	100	2	108.60	946.98	8770.34	8.72	80.76
GSBU28	2.75%	21/11/2028	9.90	100	2	113.71	1019.76	9849.79	8.97	86.62
GSBG29	3.25%	21/04/2029	10.31	100	2	119.38	1088.11	10849.51	9.11	90.88
GSBU29	2.75%	21/11/2029	10.90	100	2	115.00	1121.49	11858.25	9.75	103.11
GSBI30	2.50%	21/05/2030	11.39	100	2	112.97	1156.62	12805.93	10.24	113.35
GSBK31	1.50%	21/06/2031	12.48	100	2	102.38	1189.47	14605.35	11.62	142.66
GSBG33	4.50%	21/04/2033	14.31	100	2	142.39	1639.52	21821.17	11.51	153.25
GSBK35	2.75%	21/06/2035	16.48	100	2	121.25	1688.81	26381.19	13.93	217.58
GSBG37	3.75%	21/04/2037	18.32	100	2	140.03	2018.70	34000.34	14.42	242.81
GSBK39	3.25%	21/06/2039	20.48	100	2	134.11	2174.78	41079.53	16.22	306.32
GSBI41	2.75%	21/05/2041	22.40	100	2	127.09	2264.96	46924.53	17.82	369.23
GSBE47	3.00%	21/03/2047	28.24	100	2	137.80	2874.11	72730.63	20.86	527.82

The annuity bonds are based on Waratah Annuity Bonds (WABs) issued by the NSW government. The WABs have equal monthly base payments, and are indexed to inflation (CPI) and updated quarterly. The Waratah Annuity Bonds were discontinued in 2015, with the maturity of the on issue WABs on the market ranging from 2.79 to 5.04 years.

We use hypothetical Waratah Annuity Bonds assumed to be issued on 01/01/2019 with maturities of 5 to 40 years with sufficient duration and convexity to match the individual longevity bonds. Table 8 gives the details of the annuity bonds used in the immunization. The largest dollar duration and convexity of the WABs are 2340.95 and 63391.03, exceeding that of both individual longevity bonds.

Table 8: Details of Hypothetical Waratah Annuity Bonds.

Code	**Payment**	**Maturity**	**TTM**	**Freq**	**No. Pay**	**Price**	*Dur*	*Cov*	$\widetilde{\mathbf{D}}$	$\widetilde{\mathbf{C}}$
WAB1-21	1.00	15/10/2021	2.79	12	111	39.06	57.13	109.67	1.46	2.81
WAB2-21	1.00	15/10/2021	2.79	12	108	38.86	56.84	109.12	1.46	2.81
WAB3-22	1.00	15/01/2022	3.04	12	108	42.12	66.91	139.63	1.59	3.32
WAB4-22	1.00	15/04/2022	3.29	12	108	45.35	77.74	175.25	1.71	3.86
WAB5-22	1.00	15/07/2022	3.54	12	108	48.55	89.35	216.37	1.84	4.46
WAB6-22	1.00	15/10/2022	3.79	12	108	51.72	101.71	263.34	1.97	5.09
WAB7-23	1.00	15/01/2023	4.04	12	108	54.87	114.83	316.53	2.09	5.77
WAB8-23	1.00	15/04/2023	4.29	12	108	57.99	128.68	376.28	2.22	6.49
WAB9-23	1.00	15/07/2023	4.54	12	108	61.09	143.27	442.95	2.35	7.25
WAB10-23	1.00	15/07/2023	4.54	12	105	60.78	142.56	440.75	2.35	7.25
WAB11-23	1.00	15/10/2023	4.79	12	105	63.84	157.79	514.31	2.47	8.06
WAB12-24	1.00	15/01/2024	5.04	12	105	66.87	173.74	595.42	2.60	8.90
WAB13-24	1.00	15/01/2024	5.04	12	102	66.53	172.88	592.46	2.60	8.90
WAB14-24	1.67	15/01/2024	5.00	12	60	101.74	268.56	920.83	2.64	9.05
WAB15-29	0.83	15/01/2029	10.00	12	120	103.68	537.80	3653.67	5.19	35.24
WAB16-34	0.56	15/01/2034	15.00	12	180	105.64	820.15	8346.23	7.76	79.00
WAB17-39	0.38	15/01/2039	20.00	12	260	107.50	1113.60	15110.23	10.36	140.56
WAB18-44	0.33	15/01/2044	25.00	12	300	109.18	1415.46	24009.75	12.97	219.92
WAB19-49	0.28	15/01/2049	30.00	12	360	110.64	1722.72	35057.21	15.57	316.87
WAB20-54	0.24	15/01/2054	35.00	12	420	111.86	2032.20	48212.05	18.17	431.00
WAB21-59	0.21	15/01/2059	40.00	12	480	112.83	2340.95	63391.03	20.75	561.80

4.3 Immunization Portfolio Results

The details of the bonds selected in the hedging portfolio to immunize the liability portfolio of LCP Bond and LAI Bond are given and discussed in this section. We include immunized portfolios based on using only coupon bonds as well as using only annuity bonds. In many bond markets, including Australia, the most commonly traded government bonds are coupon bonds. In the Australian market there are annuity bonds issued by a state government. By determining and assessing portfolios based on annuity bonds we can determine the relative benefits of these compared to coupon bonds.

4.3.1 Optimal Bond Portfolios - Lifetime Coupon and Principal Bond

Table 9 gives the weights for the coupon only bond immunizing portfolio and the annuity only immunizing bond portfolio selected in the hedging portfolio to immunize the LCP Bond liability cash flows. The weights are standardized so they add up to 1 in each case.

Table 9: Bonds in the Immunized Portfolio for the LCP Bond - Coupon Bonds and Annuity Bonds.

Bond	Weight	Bond	Weight
Coupon Bonds Only			
GSBS19	0.02	GSBI28	0.02
GSBG20	< 0.01	GSBU28	< 0.01
GSBU20	< 0.01	GSBG29	0.02
GSBI21	0.01	GSBU29	0.01
GSBW21	0.01	GSBI30	0.02
GSBM22	0.01	GSBK31	0.04
GSBU22	< 0.01	GSBG33	0.09
GSBG23	0.02	GSBK35	0.07
GSBG24	0.02	GSBG37	0.07
GSBG25	0.02	GSBK39	0.12
GSBG26	0.03	GSBI41	0.03
GSBG27	0.03	GSBE47	0.35
GSBU27	0.01		
Annuity Bonds Only			
WAB2-21	< 0.01	WAB18-44	0.25
WAB15-29	< 0.01	WAB19-49	0.30
WAB16-34	0.05	WAB20-54	0.17
WAB17-39	0.13	WAB21-59	0.10

For the immunizing portfolio consisting of only coupon bonds most of the weights are allocated to longer term bonds of maturity more than 10 years reflecting the long duration of the individual longevity bond. The immunizing portfolio has 35% of the portfolio weight allocated to the bond with the longest maturity of 28.24 years ('GSBE47'), 12% to the bond with maturity of 20.48 years ('GSBK39') and less than 10% of the weight allocated to the other bonds.

For the immunizing portfolio consisting of only annuity bonds, 8 out of the 21 annuity bonds are included in the immunizing portfolio with the majority allocated to annuity bonds with maturity between 15 and 40 years, including the largest allocation of 30% of the weighting allocated to 'WAB19-49' with maturity of 30 years.

Figure 15 displays the cash flows for the LCP Bond liability and the immunizing asset portfolio for the only coupon bonds only and the only annuity bonds portfolios. We see that the annuity bond immunizing portfolio has better cash flow matching than the coupon bonds over the whole period. For the coupon bond immunizing portfolio, there are cash flow mismatches particularly between Years 15 and 30.

These comparisons are useful in visually assessing the immunizing portfolio. To compare the different bond immunizing portfolios we need to allow for interest rate reinvestment risk and to do this we will later consider the accumulated final year net cash flow surplus distributions.

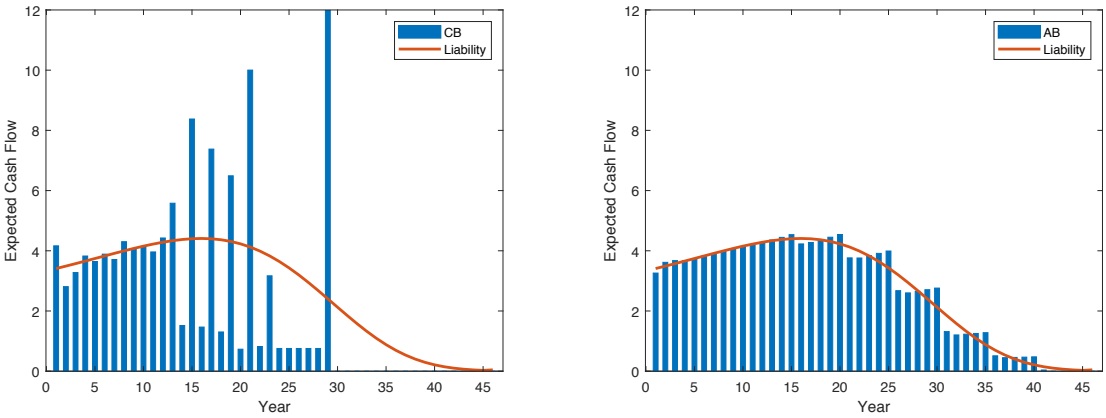

(a) Coupon Bonds (CB) Only.

(b) Annuity Bonds (AB) Only.

Figure 15: Cash Flow Match of LCP Bond, Hedged with Coupon Bonds and Annuity Bonds.

4.3.2 Lifetime Annuity Income Bond

Table 10 shows the weights for the coupon bonds and annuity bonds selected in the immunizing portfolio to hedge the LAI Bond liability. For the immunizing portfolio with only coupon bonds, as expected to reflect the expected cash flow distribution of the LAI Bond, there is a wider spread of bonds in the portfolio compared to the LCP Bond.

Table 10: Bonds in the Hedging Portfolio of LAIB.

Bond	Weight	Bond	Weight
Coupon Bonds Only			
GSBS19	0.06	GSBI28	0.03
GSBG20	< 0.01	GSBU28	0.01
GSBU20	0.02	GSBG29	0.02
GSBI21	0.03	GSBU29	0.02
GSBW21	0.02	GSBI30	0.03
GSBM22	0.02	GSBK31	0.05
GSBU22	0.00	GSBG33	0.11
GSBG23	0.04	GSBK35	0.06
GSBG24	0.05	GSBG37	0.07
GSBG25	0.04	GSBK39	0.05
GSBG26	0.05	GSBI41	0.06
GSBG27	0.05	GSBE47	0.10
GSBU27	0.01		
Annuity Bonds Only			
WAB2-21	0.03	WAB18-44	0.19
WAB13-24	0.04	WAB19-49	0.13
WAB15-29	0.14	WAB20-54	0.05
WAB16-34	0.18	WAB21-59	0.02
WAB17-39	0.22		

For the immunizing portfolio with only annuity bonds, a slightly higher number of 9 annuity bonds are selected from a total of 21 bonds as compared to the LCP Bond. Also, as expected, the weights are more spread for this portfolio.

The cash flows for the immunizing bond portfolios for the LAI Bond are displayed in Figure 16. For the coupon bond portfolio, there is a cash flow mismatch mainly between years 15 to

30, highlighting the potential reinvestment risk compared to the annuity bond portfolio. Once again, the annuity bond portfolio cash flows show a closer match than the coupon bond portfolio cash flows.

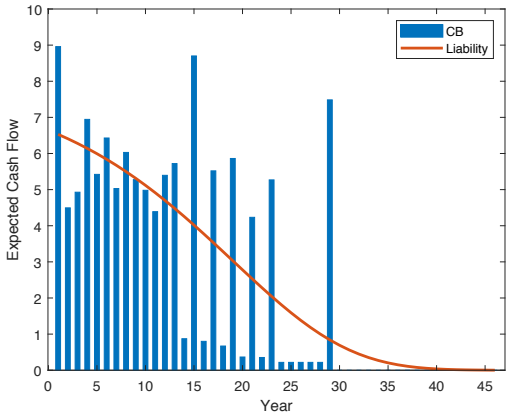

(a) Coupon Bonds (CB) Only.

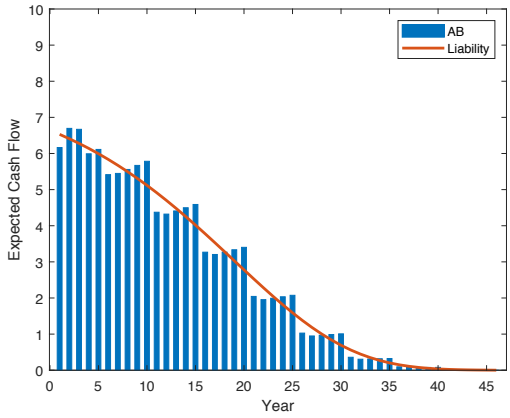

(b) Annuity Bonds (AB) Only.

Figure 16: Cash Flow Match of LAIB, Hedged with Coupon Bonds and Annuity Bonds.

4.4 Portfolio Surplus Distribution

Although the cash flows show that the annuity bonds have a closer cash flow match, to provide an assessment of the effectiveness of immunizing bond portfolio allowing for reinvestment risk, we consider the distribution of the final year surplus of the net cash flows. The final year is at time $t = 46$ after which there are no more individual longevity bond cash flows. To do this we simulate paths for the interest rates and mortality rates using the transition equations for the risk factors L_t, S_t and C_t. The monthly net cash flows (NCF_t^j) are then compounded to the end of the time period at stochastic interest rates, to produce the accumulated net cash flow:

$$NCF_t^j = CF_t(\text{Asset}) - \left(\mathcal{S} \times S^j(0,t) + \mathcal{D} \times \left(S^j(0,t-\frac{1}{12}) - S^j(0,t)\right)\right),$$

$$\text{Surplus}_{46}^j(NP) = \sum_{t\geq 0}^{46} \frac{NCF_t^j}{D^j(t,46)},$$

where j stands for the j^{th} simulation.

Figure 17 compares the simulated final year surplus distribution of the un-hedged portfolio, the portfolio immunized only with coupon bonds, and the portfolio immunized only with annuity bonds for both the LCP Bond and LAI Bond.

Surprisingly, but also reflecting the results in Liu and Sherris (2017), we see that the difference in the final year surplus distribution between the immunizing portfolios with only coupon bonds and only annuity bonds is small despite the expected cash flow differences. The final year surplus distribution of the LCP Bond is more effectively hedged than that of the LAI Bond. This reflects the results in Table 6 where the LCP Bond has higher interest rate risk due to the larger payments at older ages. The distribution of the final year surplus of the LCP Bond is narrower than that of the LAI Bond, reflecting a lower level of longevity risk in the LCP Bond portfolio arising from the natural hedging in the bond cash flows.

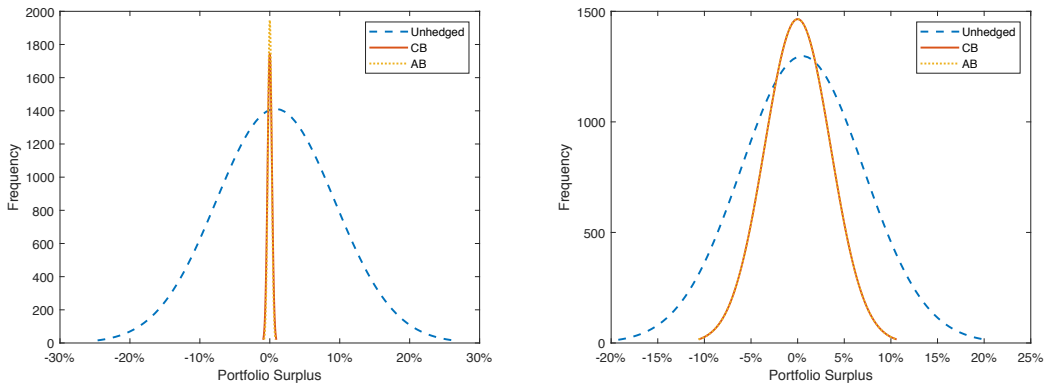

(a) LCP Bond. (b) LAI Bond.

Figure 17: Final Year Surplus Distribution of Un-hedged Portfolio, Portfolio Hedged with Coupon Bonds (CB) and Annuity Bonds (AB).

We use the $\text{VaR}_{0.5\%}$ of the final year surplus distribution to quantify the hedging effectiveness of the immunized bond portfolios and to assess the loading required in the individual longevity bond prices. Results are displayed in Table 11 below:

Table 11: Comparison of Final Year Surplus Distribution $\text{VaR}_{0.5\%}$.

	Un-hedged	Hedged with CB	Hedged with AB
$\text{VaR}_{0.5\%}$(LCP Bond)	-26.47%	-0.95%	-0.89%
$\text{VaR}_{0.5\%}$(LAI Bond)	-14.71%	-9.92%	-9.91%

Table 11 shows the extent to which the immunization reduces the final year $\text{VaR}_{0.5\%}$ for both the LCP Bond and the LAI Bond. Both individual longevity bonds when immunized with only annuity bonds have slightly lower $\text{VaR}_{0.5\%}$ compared to the portfolio with only coupon bonds. The difference in the $\text{VaR}_{0.5\%}$ is not very significant, so that although a benefit of using annuity bonds is the better cash flow match, the coupon bonds are also effective in immunizing the interest rate risk in the individual longevity bonds. This confirms the results in Liu and Sherris (2017).

For the immunized portfolios, the VaR can be used to asses the price loading for systematic longevity risk and the residual interest rate risk. Based only on the final year surplus, these results show that for the LCP Bond a loading of approximately 1% to the bond price would be appropriate, and for the LAI Bond a loading of approximately 10% would be appropriate. The Flexible Bond loading is a weighted average of these. The significantly lower VaR of the LCP Bond quantifies the benefits of natural hedging in the LCP Bond design. Since the LCP bond pays an approximately interest only market coupon reflecting market yields and a mortality credit and a return of principal on death, then regardless of the date of death the value of the bond will be approximately equal to the principal.

5 Longevity Risk Loading and SPV Capital Requirement

Since there are no wholesale longevity bonds issued by governments in the Australian market, as is the case in most countries, we need to assess the capital requirements for the individual longevity bonds for the special purpose vehicle and to do this we adopt a Solvency II approach.

Having quantified the capital requirements we use this to assess the longevity risk loading in the price of the individual longevity bonds.

5.1 Systematic Mortality Risk - Solvency Capital Requirement and Risk Margin

The special purpose vehicle will hold capital for the risks in the immunized portfolio, which is mainly longevity risk. We determine the capital requirement using the Solvency Capital Requirement (SCR) under Solvency II, which is defined as the capital an insurer needs to hold to survive a 1 in 200 year permanent shock to the mortality rate (EIOPA, 2011). A standard formula for calculating SCR is:

$$SCR_t := NAV_t - (NAV_t|\text{Mortality Shock}),$$

where NAV_t stands for net asset value at time t (Meyricke and Sherris, 2014).

In practice, the SCR_t is usually approximated. We approximate the SCR_t by using our models to simulate the distribution of the net asset value NAV_t for each time t and determining the 1 in 200 year mortality shock as the 0.5% value-at-risk of the NAV_t distribution.

The NAV_t reflects the risk from time t onwards, so the distribution of NAV_t is constructed with the expected value of simulated cash flows and interest rates before time t, and stochastic cash flows and interest rates after time t, using:

$$NAV_t^j = \sum_{n=0}^{t} \frac{NCF_n}{D(n,t)} + \sum_{n=t+1}^{46} NCF_n^j \times D^j(t,n),$$

where NCF stands for the expected net cash flow, and NCF^j stands for the j^{th} simulated net cash flow.

Then the solvency capital requirement SCR_t that the special purpose vehicle holds at time t $(t = 0, 1, 2, ...)$ is given by:

$$SCR_t = \text{mean}(NAV_t) - \text{VaR}_{0.5\%}(NAV_t),$$

where the mean and $\text{VaR}_{0.5\%}$ are taken from the simulated distribution of NAV_t.

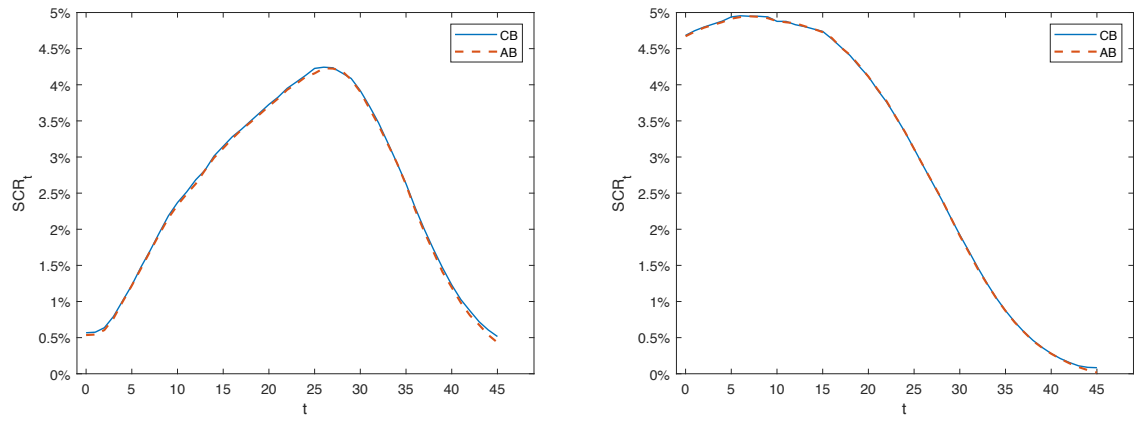

(a) LCP Bond.

(b) LAI Bond.

Figure 18: Solvency Capital Requirement over Time. Hedged with Coupon Bonds (CB) or Annuity Bonds (AB).

The computed SCR_t for the LCP Bond and LAI Bond is shown in Figure 18(a) and Figure 18(b) respectively. For the LCP Bond, the SCR_t is low at time $t = 0$ due to the natural hedging effect. Then with the natural hedging effect decreasing over time, the SCR_t increases for the next 25 years or so. After that, the SCR_t gradually reduces to zero until the end of the liability cash flows. For the LAI Bond with only a survival annuity benefit, the SCR_t gradually decreases over time until it reaches zero. There are no large differences between the immunizing portfolios with only coupon bonds (CB) and only annuity bonds (AB).

5.2 Risk Margin

A risk margin (RM) needs to be included in the bond pricing for the longevity and residual interest rate risk in the immunizing portfolios. At the beginning of each year, the cost of holding capital is the cost of capital (CoC) times the solvency capital requirement (SCR_t) at that time. The risk margin is determined as the expected present value of all the capital costs at time 0, given by:

$$RM = \sum_{t=0}^{\infty} CoC \times SCR_t \times D(0,t), \quad \text{where } CoC = 6\% \text{ under Solvency II.}$$

The special purpose vehicle will need to determine a solvency risk margin. We determine this as a proportion of the price of the bonds (EPV) to cover the RM, using:

$$EPV + RM = EPV \times (1 + \text{Loading}), \quad \text{Loading} = \frac{RM}{EPV}.$$

The risk margins for the LCP Bond and LAI Bond are shown in Table 12. The risk margins for the LCP Bond, based on the immunizing portfolio with only CB and only AB, are 5.08% and 5.02% respectively, which are 1.80 and 1.85 percentage points lower than the loadings for the LAI Bond. The lower required risk margins for the LCP Bond reflects the benefit of the natural hedging built into the bond cash flows with both survival benefits and a death benefit. The solvency risk margins based on the (CoC) approach differ from the VaR of the final year surplus distribution because they consider each year throughout the time period of the bond rather than the final period only. They also reflect the actual capital that the SPV will be required to hold. As such they give a better indication of the loading required in the individual bond prices for systematic longevity risk.

Table 12: Required Loading for LCP Bond and LAI Bond.

	$\text{Loading}_{\text{CB}}$	$\text{Loading}_{\text{AB}}$
Lifetime Coupon and Principal Bond (W=100)	5.08%	5.02%
Lifetime Annuity Income Bond (W=0)	6.88%	6.87%

We also show the risk margins of the Flexible LIP Bond^W, with W% of weights in the LCP Bond and $(1 - W\%)$ weights in the LAI Bond, for different W in the LCP Bond in Figure 19.

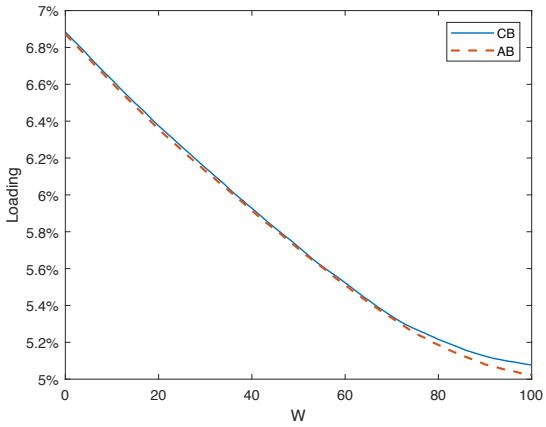

Figure 19: Loading of the Flexible LIP Bond^W with Different W. Hedged with Coupon Bonds (CB) or Annuity Bonds (AB).

The Flexible LIP Bond^W allows individuals to base the survival benefit and the death benefit in their preferences by varying the weighting factor W. As W increases, the bond price loading decreases approximately linearly, reflecting the benefits from the the natural hedging in the LCP Bond.

6 Conclusions

We have proposed new individual longevity bonds that allow individuals to more flexibly manage their longevity risk compared to currently available products such as life annuities. They allow an individual to determine a level of bond income while alive as well as a principal payment on death providing a bequest that reflects their individual preferences. The bonds are a weighted combination of a lifetime coupon and principal bond (LCP Bond) and a lifetime annuity income bond (LAI Bond). We provide a detailed analysis and assessment of these standardized longevity bonds that form the basis for a flexible range of bonds by mixing different weights of these bonds.

We present the financial engineering underlying the pricing and risk management of the bonds. To do this we calibrate independent AFNS interest rate and AFNS mortality models using Australian data. Both models have an excellent fit to the data and are well-suited for financial and actuarial engineering applications including the pricing and risk management of the individual longevity bonds as well as for simulating future interest rate and mortality scenarios. We determine and assess the immunizing hedging portfolio of Australian government bonds for the interest rate risk in the individual longevity bond liability portfolio. We also consider the price loading required for the longevity risk and residual interest rate risk in the individual bonds that cannot be immunized, mostly reflecting systematic longevity risk. Although we use Australian data and the Australian bond market, the models and results are applicable to any country with a developed interest rate and bond market and aggregate mortality data.

We show that an immunized bond portfolio fully collateralized with standard coupon paying government bonds is effective in hedging interest rate risk for these individual longevity bonds. If government issued annuity bonds were available, then these would provide a better cash flow matching for the expected cash flows on the individual longevity bonds. There is also little difference in value-at-risk in the final year accumulated net cash flow surplus distribution for the immunizing portfolios based on only coupon bonds as opposed to only annuity bonds.

We assess the price loadings required for the LCP Bond and for the LAI Bond. We consider

both final year portfolio surplus and regulatory capital requirements. There is a lower loading for the LCP Bond because of the natural hedging included in the product cash flows with both a survival income benefit and principal payment on death.

Although we do not focus on the individual mortality assumptions required to reflect adverse selection for the bonds, this can be readily included as margins to the aggregate mortality model. Our focus has been on the aggregate mortality risk and the application of financial and actuarial engineering including a recently developed age-cohort mortality model well suited for this application. Since individuals are allowed to select a flexible bond to reflect their bequest preferences, this also mitigate potential adverse selection.

7 Acknowledgement

The authors acknowledge financial support from the Society of Actuaries Center of Actuarial Excellence Research Grant 2017–2020: Longevity Risk: Actuarial and Predictive Models, Retirement Product Innovation, and Risk Management Strategies as well as support from CEPAR Australian Research Council Centre of Excellence in Population Ageing Research project number CE170100005.

References

Biffis, E. (2005). Affine processes for dynamic mortality and actuarial valuations. *Insurance: Mathematics and Economics*, 37(3):443–468.

Blackburn, C. and Sherris, M. (2013). Consistent dynamic affine mortality models for longevity risk applications. *Insurance: Mathematics and Economics*, 53(1):64–73.

Blake, D. and Burrows, W. (2001). Survivor bonds: Helping to hedge mortality risk. *Journal of Risk and Insurance*, 68(2):339–339.

Blake, D., Cairns, A. J., and Dowd, K. (2006). Living with mortality: Longevity bonds and other mortality-linked securities. *British Actuarial Journal*, 12(1):153–197.

Brown, J. R. (2009). Understanding the role of annuities in retirement planning. In Lusardi, A., editor, *Overcoming the Saving Slump: How to Increase the Effectiveness of Financial Education and Saving Programs*, pages 178–206. University of Chicago Press.

Christensen, J., Diebold, F., and Rudebusch, G. (2011). The affine arbitrage-free class of Nelson–Siegel term structure models. *Journal of Econometrics*, 164(1):4–20.

Dahl, M. (2004). Stochastic mortality in life insurance: market reserves and mortality-linked insurance contracts. *Insurance: Mathematics and Economics*, 35(1):113–136.

De Jong, P. and Ferris, S. (2019). SM bonds: A new product for managing longevity risk. *Journal of Risk and Insurance*, 86(1):121–149.

Duffie, D. and Kan, R. (1996). A yield-factor model of interest rates. *Mathematical Finance*, 6(4):379–406.

EIOPA (2011). European insurance and occupational pension authority (EIOPA) report on the fifth Quantitative Impact Study (QIS5) for Solvency II. Technical report.

Evans, J. and Sherris, M. (2010). Longevity risk management and the development of a life annuity market in Australia. Research Paper 2010ACTL01, Australian School of Business.

Huang, Z., Sherris, M., Villegas, A., and Ziveyi, J. (2019). The application of affine processes in cohort mortality risk models. Research paper, UNSW Business School. Available at SSRN 3446924.

Hyndman, R. J. and Koehler, A. B. (2006). Another look at measures of forecast accuracy. *International Journal of Forecasting*, 22(4):679–688.

Liu, C. and Sherris, M. (2017). Immunization and hedging of post retirement income annuity products. *Risks*, 5(1):19.

Luciano, E., Regis, L., and Vigna, E. (2012). DeltaŰgamma hedging of mortality and interest rate risk. *Insurance: Mathematics and Economics*, 50(3):402 – 412.

Meyricke, R. and Sherris, M. (2014). Longevity risk, cost of capital and hedging for life insurers under Solvency II. *Insurance: Mathematics and Economics*, 55:147–155.

Modigliani, F. (1986). Life cycle, individual thrift, and the wealth of nations. *Science*, 234(4777):704–712.

Panjer, H. H., Boyle, P. P., Cox, S. H., Dufresne, D., Gerber, H., Mueller, H., Pedersen, H., Pliska, S., Sherris, M., Shiu, E., et al. (1998). *Financial Economics: With Applications to Investments, Insurance, and Pensions*. Actuarial Foundation Schaumburg, Ill.

Schrager, D. F. (2006). Affine stochastic mortality. *Insurance: Mathematics and Economics*, 38(1):81–97.

Willis Towers Watson (2018). Global pension assets study 2018. *Willis Towers Watson*.

Xu, Y., Sherris, M., and Ziveyi, J. (2019). Continuous-time multi-cohort mortality modelling with affine processes. *Scandinavian Actuarial Journal*, 0(0):1–27.

Yaari, M. E. (1965). Uncertain lifetime, life insurance, and the theory of the consumer. *Review of Economic Studies*, 32(2):137–150.